Nucleic Acids Research, 2025, **53**, gkaf703
https://doi.org/10.1093/nar/gkaf703
Synthetic Biology and Bioengineering

Genetic "expiry-date" circuits control lifespan of synthetic scavenger bacteria for safe bioremediation

Kha Mong Tran [1], Nuong Thi Nong [1], Jun Ren [1], Kangseok Lee [2], Doheon Lee [3], Jörg Gsponer [4], Hyang-Mi Lee [1,*], Dokyun Na [1,*]

[1]Department of Biomedical Engineering, Chung-Ang University, 84 Heukseok-ro, Dongjak-gu, Seoul 06974, Republic of Korea
[2]Department of Life Science, Chung-Ang University, 84 Heukseok-ro, Dongjak-gu, Seoul 06974, Republic of Korea
[3]Department of Bio and Brain Engineering, KAIST, 291 Daehak-ro, Yuseong-gu, Daejeon 34141, Republic of Korea
[4]Department of Biochemistry and Molecular Biology, University of British Columbia, 2125 East Mall, Vancouver, BC V6T 1Z4, Canada

*To whom correspondence should be addressed. Email: blisszen@cau.ac.kr
Correspondence may also be addressed to Hyang-Mi Lee. Email: myhys84@cau.ac.kr

Abstract

Synthetic biology enabled the systematic engineering of bacteria for diverse applications, but their deployment in open environments raises concerns about their persistence and unintended ecological impacts. To address these challenges, genetic "expiry-date" circuits were designed to impose a tunable lifespan on bacteria. These circuits, structured as a feedforward activation network, regulate the timing of cell death by controlling the expression of Lysis E, enabling a programmed lifespan ranging from hours to days. The lifespan can be tailored by modifying the number of activation steps in the cascade. The circuits were optimized by reducing gene expression leakiness of Lysis E using a synthetic small regulatory RNA and combining it with an *asd*-based auxotrophic system. The bacteria harboring the "expiry-date" circuits resulted in a GMO escape rate below U.S. NIH release standards ($<10^{-10}$). To validate the practical applicability of this system, a synthetic phenol-scavenging *Escherichia coli* was constructed, which possessed enhanced phenol tolerance and phenol-detoxification capability, and harbored the "expiry-date" circuits. The engineered bacteria detoxified 0.1 g/kg of phenol in soil within 4 days and self-destructed by day 5. These results support the circuit's potential as a biocontainment strategy for the safe and controlled deployment of synthetic bacteria in real-world applications.

Graphical abstract

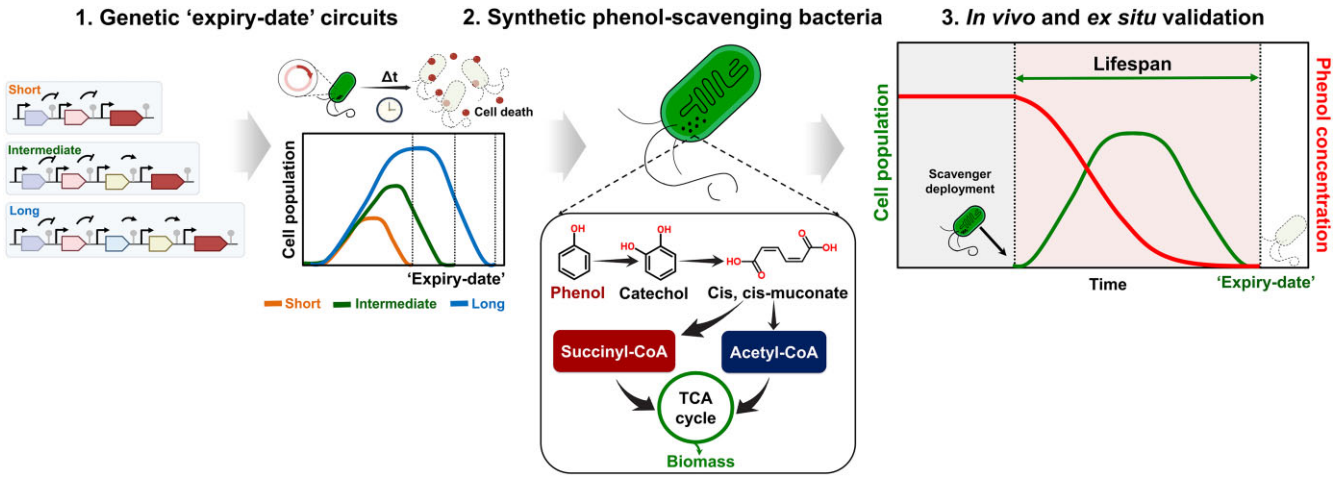

Introduction

In recent years, the robust development of synthetic biology has enabled the deciphering and redesigning of cellular systems in biotechnology. Genetic tools developed in synthetic biology allow for the redesign of metabolic pathways and the regulation of these pathways through synthetic genetic circuits in an orchestrated and finely controlled manner [1–3]. These advancements have facilitated the utilization of synthetic bacteria in diverse biotechnology fields such as biorefineries, drug delivery [4, 5], biomaterials fabrication [6, 7], bioremediation [8, 9], etc. [10–13].

Received: April 6, 2025. **Revised:** July 1, 2025. **Editorial Decision:** July 2, 2025. **Accepted:** July 8, 2025

The employment of synthetic bacteria in biomedical and biotechnological applications raises ongoing concerns. These concerns stem from the potential harm they might pose to indigenous microbes and other living organisms, including humans, as well as the potential disruption of ecosystems through unintended growth [14]. The release of engineered synthetic bacteria into the human body for biomedical purposes exemplifies these issues. For example, therapeutic synthetic bacteria could proliferate uncontrollably within the human body, releasing toxic by-products and potentially causing sepsis [15]. Therefore, it is imperative that therapeutic bacteria are effectively eliminated after completing their programmed mission [16–18]. Similarly, the deployment of synthetic bacteria for bioremediation in open environments raises concerns about unintended environmental risks. While numerous studies have focused on engineering environmentally friendly strains [19], they may not fully address the need for robust biocontainment strategies to prevent the unintended spread of engineered bacteria. Their uncontrolled proliferation in contaminated areas could disrupt ecosystems by outcompeting native microbial populations [20].

To address these challenges, several biocontainment strategies have been implemented to prevent the unintended proliferation of synthetic bacteria. Previous studies have utilized genetic circuits to regulate the expression of essential genes [21] or toxin genes under defined conditions [22]. Upon the loss of permissive conditions, these circuits either suppress essential gene expression or activate toxin gene expression, leading to cell death. Notable examples of such strategies include CRISPR–Cas9 kill switches [23], synthetic auxotrophic strains reliant on specific compounds [24–26], or a combination of both approaches [27].

These pioneering methods, however, face significant challenges, including regulatory leakiness [28] and environmental instability [29], which may compromise their reliability. Furthermore, their practical application outside laboratory settings remains limited as they often require human intervention and external stimuli (such as chemical or physical inducers) to trigger cell death [21, 23, 30–34]. Moreover, the constrained scalability of these strategies hinders their ability to provide synthetic bacteria with diverse, tunable lifespans. Therefore, developing a robust and easily expandable genetic system to control bacterial lifespan or impose an "expiry-date" is essential.

In this study, we constructed a genetic "expiry-date" circuit that triggers a self-destruct sequence upon deployment in open environments. This circuit consists of a series of transcriptional activation steps, ultimately leading to the expression of a self-destruct gene. In laboratory settings, this cascade is inhibited by a chemical blocker, but once released into an environment where the blocker is absent, the sequence is initiated. The lifespan of synthetic bacteria is controlled by the number of transcriptional activation steps, allowing for tunable time delays. To demonstrate this approach, we constructed three genetic "expiry-date" circuits with different lifespans: short, intermediate, and long "expiry-date" networks. In engineered *Escherichia coli* (*E. coli*), the programmed lifespan ranged from several hours to several days, depending on initial cell density and environmental conditions, including M9 media for *in vivo* validation and nutrient-poor soil for *ex situ* validation.

For the practical application of the genetic "expiry-date" circuit, we developed a synthetic scavenger *E. coli* capable of degrading phenol pollutants [35], even at high concentrations. Bacteria play an increasingly important role in bioremediation, providing a sustainable alternative to chemical methods for pollutant degradation. Compared with chemical treatments, biological approaches using microbes often require fewer resources and generate fewer secondary pollutants, making them more environmentally friendly. Due to safety concerns, previous phenol bioremediation efforts have primarily relied on naturally occurring bacteria [36–40]. However, most of these attempts have largely been ineffective, as most natural strains prioritize survival in toxic environments over efficient contaminant removal. While there is a continuous demand for engineered bacteria with enhanced bioremediation efficiency, concerns over the environmental risks of releasing synthetic organisms have hindered their real-world applications. To address these biosafety challenges, we integrated the genetic "expiry-date" circuit into the phenol-degrading synthetic scavenger *E. coli,* enabling its programmed self-elimination after a defined lifespan. When equipped with an intermediate "expiry-date" circuit, the synthetic scavenger *E. coli* successfully degraded 0.1 g/kg of phenol in soil and became undetectable after 5 days, confirming complete removal. The modular and flexible nature of this genetic circuit makes it highly adaptable for industrial and biotherapeutic applications.

Materials and methods

Strains, plasmids, media, and genome modification

We used *E. coli* NEB Turbo for conventional gene cloning. Various *E. coli* strains—including BL21 (DE3), SURE, LS5218, JM109, and MK01—were evaluated for phenol tolerance. All strains were cultivated in Luria-Bertani (LB) medium supplemented with appropriate antibiotics for phenol tolerance assays. For assessing genetic "expiry-date" circuits and evaluating the phenol degradation efficiency of synthetic scavenger strains, we used M9 minimal medium supplemented with 2 mM $MgSO_4$, 100 μM $CaCl_2$, 30 μM $FeSO_4$, 1 mM EDTA, 0.5% (w/v) glycerol, 0.2% (w/v) casamino acids, and appropriate antibiotics. The antibiotics used included ampicillin (100 μg/mL), chloramphenicol (34 μg/mL), kanamycin (50 μg/mL), and spectinomycin (100 μg/mL).

We constructed *meso*-2,6-diaminopimelic acid (DAP)–auxotrophic strains by disrupting the essential *asd* gene using the CRISPR RNA-guided integrase from the pSPIN system (Addgene #160729) [41]. We supplemented the culture medium with 0.1 mM DAP to grow DAP–auxotrophic strains.

Plasmid construction

To enhance phenol tolerance, we amplified the *rpoD* and *secB* genes from the genome of *E. coli* DH5α and cloned them into the pWA plasmid [42]. We generated mutant variants, $secB^{T10A}$ and $rpoD^{C9}$ via site-directed mutagenesis. For constructing a synthetic phenol-degradation metabolic pathway, we cloned operons encoding pathway enzymes into plasmids as follows: the *cat* operon (*catB*, *catC*, and *catA1*) from *Pseudomonas putida* KT2440 and the *pheA2* and *pheA1* genes from *Rhodococcus erythropolis* KCTC 3483 were cloned into the pColE1 plasmid, while the *pca* operon (*pcaF*, *pcaD*, *pcaI*, and *pcaJ*) from *P. putida* KT2440 was cloned into the p15A plasmid. All these genes were expressed under the control of a synthetic promoter (J23119).

We cloned genes used for the genetic "expiry-date" circuits from the genome of *E. coli* DH5α, the pZS1-lTlrLLtCL3 plasmid [43] (Addgene #26489), the pTD103luxI-sfGFP plasmid [44] (Addgene #48885), and the ePop plasmid [45] (Addgene #50953). We introduced appropriate mutations into transcription regulator genes via site-directed mutagenesis. The genetic circuits were constructed in a pSC101 plasmid. To reduce leaky expression of the lysis gene *E*, we designed a synthetic anti-Lysis E sRNA (synthetic small regulatory RNA) as previously described [46]; the sRNA gene was placed under the control of the $P_{LtetO-1}$ promoter. For the growth of *asd*-deleted *E. coli* strains without DAP supplementation, we amplified the *asd* gene from *E. coli* genome and placed it under the control of a weak promoter, J23106, to provide plasmid stabilization. The sRNA and *asd* gene were integrated into the pSC101 plasmid containing the genetic "expiry-date" circuit.

Evaluation of activity and inducer dependency of transcriptional regulators

To assess the activity and inducer dependency of transcriptional regulators (CI repressor, AraC activator, and LuxR activator) and their variants (CI^{857}, CI^{ts2}, $AraC^{L9P}$, $AraC^{T13H}$, $AraC^{V20M}$, $LuxR^{A221V}$, and $LuxR\Delta_{2-162}$), *E. coli* cells harboring the regulators and the *egfp* gene encoding Enhanced Green Fluorescent Protein (EGFP) under the control of the respective promoters were grown overnight in LB medium. Cultures were washed with sterilized phosphate-buffered saline (PBS, pH 7.4) buffer and diluted to 1% in fresh M9 minimal medium supplemented with appropriate antibiotics. The cultures were incubated at 25°C and 230 rpm until reaching an optical density at 600 nm (OD_{600}) of 0.4–0.5. Cells were then induced with appropriate inducers for 12 h at 25°C and 230 rpm: 100 nM anhydrotetracycline (aTc) for testing CI repressors with the P_R promoter, 0.2% L-arabinose for testing AraC activators with the P_{BAD} promoter, and 1000 nM N-(3-oxohexanoyl) homoserine lactone (3OC6-HSL) for testing LuxR activators with the P_{lux} promoter. After induction, 500 μL of cultures were collected, centrifuged at 7000 rpm for 10 min, washed twice, and resuspended with sterilized PBS. Cells were diluted 1% (v/v) into fresh PBS for analysis. EGFP intensity was measured using a Millipore Guava easyCyte High-Throughput Flow Cytometer with a 488 nm excitation laser and a 515 nm emission filter. At least 10 000 events were collected per sample.

Functionality assay of genetic "expiry-date" circuits

Colonies of *E. coli* strains harboring plasmids with a genetic "expiry-date" circuit were grown overnight in M9 minimal medium supplemented with 100 nM aTc and appropriate antibiotics at 25°C with shaking at 230 rpm until reaching an OD_{600} of 0.4–0.5. To initiate the genetic "expiry-date" circuits, cultures were washed four times with sterilized PBS to remove residual aTc and diluted to an OD_{600} of 0.01 in fresh M9 minimal medium with antibiotics.

For the kinetic growth assay, optical density at 600 nm was measured every 30 min over 36 h using a Synergy™ H1 hybrid multi-mode microplate reader (BioTek) at 25°C with continuous shaking. A 96-well plate with a transparent flat bottom and adhesive film was used. The "death phase" was defined as the point where the OD_{600} reached its maximum before declining.

For the survival ratio assay, samples from the kinetic growth assay were collected at 12, 24, 36, and 48 h, serially diluted in PBS, and plated onto LB agar containing 100 nM aTc. Plates were incubated at 25°C for 40–48 h to enumerate colony-forming units (CFUs). Survival ratios were calculated using Equation (1):

$$\mathrm{Log}_{10}(\text{Survival ratio}) = \mathrm{Log}_{10}\left(\frac{\text{CFU/mL without aTc}}{\text{CFU/mL with aTc}}\right) \quad (1)$$

For long-term circuit stability testing, cells were passaged under survival conditions (100 nM aTc) for 14 times. Every 24 h, diluted cells (100-fold) were transferred to fresh media and incubated for another 24 h. Every 48 h, CFU was quantified to assess circuit stability by incubating cells in the presence or absence of aTc.

Phenol tolerance assay

Phenol tolerance was assessed by measuring the growth of *E. coli* strains in LB medium containing varying concentrations of phenol (0, 0.25, 0.5, 1.0, 1.5, and 2.0 g/L). Five *E. coli* strains—BL21 (DE3), SURE, LS5218, JM109, and MK01—were inoculated into LB medium and incubated overnight at 37°C with shaking at 230 rpm. The overnight cultures were then diluted 1% (v/v) into fresh LB medium and incubated under the same conditions until the OD_{600} reached 0.4–0.5.

For phenol tolerance testing, each strain was exposed to the specified phenol concentrations in LB medium. Growth was monitored at 30-min intervals over 24 h using a Synergy™ H1 hybrid multi-mode microplate reader (BioTek, Vermont, USA) at 25°C in a 96-well plate format. Phenol tolerance was determined by comparing growth in the presence and absence of phenol, calculated using Equation (2):

$$\text{Phenol tolerance}(\%) = \frac{(OD_{600}\text{ at 24h} - OD_{600}\text{ at 0h})\text{ in the presence of phenol}}{(OD_{600}\text{ at 24h} - OD_{600}\text{ at 0h})\text{ in the absence of phenol}} \times 100 \quad (2)$$

Additionally, the growth rate (μ) of strains during the exponential phase was calculated using Equation (3):

$$\mu = \frac{In\,OD_2 - In\,OD_1}{t_2 - t_1} \quad (3)$$

where t_1 and t_2 are two sampling time points, and OD_1 and OD_2 are the respective optical densities at 600 nm [47].

Phenol tolerance assays for the engineered MK01 strains expressing $rpoD^{C9}$, $secB^{T10A}$, or both proteins were conducted under the same conditions as those for the various *E. coli* strains.

Phenol biodegradation assay

For the phenol biodegradation assay conducted in flasks, seed cultures of the strain harboring the plasmids for the phenol-degrading pathway and $rpoD^{C9}$ were grown overnight in LB medium at 37°C with shaking at 230 rpm. After incubation, the cultures were washed with sterilized PBS and resuspended to an OD_{600} of 2.0 in 100 mL of fresh M9 minimal medium with appropriate antibiotics. Various phenol concentrations (0.1, 0.3, 0.5, 1.0, and 1.5 g/L) were then introduced to evaluate the biodegradation capabilities of the transformed strains. The cultures were incubated at 25°C with shaking at 230 rpm. Samples were collected periodically to monitor both

cell growth and residual phenol concentration. After sampling, cultures were centrifuged, and the cell-free supernatants were analyzed for residual phenol concentration using high-performance liquid chromatography (HPLC).

Estimation of the time for complete phenol degradation

To estimate the time required for complete phenol degradation at higher concentrations (1.0 and 1.5 g/L) using the *E. coli* MK01 strain, we fitted the measured phenol concentrations and corresponding degradation times to linear regression models. For 1.0 g/L phenol, the extrapolated time for complete phenol elimination was determined using Equation (4):

$$y = -0.006420x + 0.9426 (R^2 = 0.7873) \quad (4)$$

Similarly, for 1.5 g/L phenol, the extrapolated time was calculated using Equation (5):

$$y = -0.007598x + 1.466 (R^2 = 0.9366) \quad (5)$$

In vivo assay of genetic "expiry-date" circuits in phenol-degrading *E. coli* MK01

Seed cultures of phenol-degrading *E. coli* MK01Δ*asd* strains harboring genetic "expiry-date" circuits were grown overnight in 5 mL of M9 minimal medium at 25°C with shaking at 230 rpm, supplemented with 100 nM aTc. Cultures were harvested by centrifugation at 7000 rpm for 15 min, washed four times with sterilized PBS buffer to remove residual aTc, and resuspended to an OD_{600} of 2.0 in 100 mL of fresh M9 minimal medium in flasks. To maintain plasmids, antibiotics were added to the medium: chloramphenicol (34 μg/mL), ampicillin (100 μg/mL), kanamycin (50 μg/mL), and spectinomycin (100 μg/mL). Various phenol concentrations (0.1, 0.3, and 0.5 g/L) were introduced to evaluate the biodegradation capabilities of the synthetic phenol scavengers at 25°C with shaking at 230 rpm. One milliliter of culture was collected every 2 h, centrifuged, and the supernatant was retained for phenol analysis to enable detailed tracking of degradation over time. To assess viable cell counts, 100 μL of culture was collected every 6 h, serially diluted in sterilized PBS, and spread on LB agar plates supplemented with 100 nM aTc and appropriate antibiotics. Plates were incubated at 25°C for 40–48 h, and colonies were enumerated. The viable cell count was calculated as $\log_{10}$ (CFU/mL) for each sample.

Ex situ bioremediation assay

The *ex situ* bioremediation assay was conducted using natural soil sourced from Northern Aggregate in Daegu, Korea. To confirm the absence of phenol in the purchased soil samples, 1 g of soil was suspended in 1 mL of sterilized deionized water in a 15 mL conical tube. The tube was vortexed for 1 min and centrifuged at 4000 rpm for 15 min. After centrifugation, 1 mL of the supernatant was collected, filtered through a 0.22 μm filter, and analyzed for phenol content using HPLC. To eliminate interference from indigenous microorganisms, the soil was sterilized by autoclaving at 121°C and 1.4 bar for 2 h. This sterilization process was repeated three times over 48 h to ensure complete elimination of native microbial communities.

A phenol stock solution (50 g/L) was diluted by adding 5 mL into 95 mL of sterilized distilled water. This diluted solution was used to contaminate 2.5 kg of sterilized soil, achieving a target phenol concentration of 0.1 g/kg soil, corresponding to moderate contamination levels typically observed in natural soil or groundwater [48]. Phenol loading was confirmed using HPLC. The contaminated soil was divided into 200 g samples in Duran bottles for each treatment.

Each strain was cultivated overnight in 5 mL of M9 minimal medium supplemented with 100 nM aTc at room temperature with shaking at 230 rpm. Cultures were pelleted by centrifugation at 7000 rpm for 15 min, washed four times with PBS to remove residual aTc and trigger the genetic "expiry-date" circuits, and resuspended in fresh PBS to a final density of 10^7 CFU/g soil, ensuring sufficient bacterial deployment for standard *ex situ* soil bioremediation assays [49, 50]. For the control (*E. coli* MK01Δ*asd* without any plasmids), 0.1 mM DAP was added to the soil to support cell viability. Uninoculated Duran bottles were maintained as abiotic controls. The soil moisture content was adjusted to 60% of the water-holding capacity to facilitate aerobic biodegradation [51]. The Duran bottles were thoroughly mixed, sealed, and incubated at 25°C for 30 days.

One gram of soil was collected periodically to analyze residual phenol concentrations and viable cell counts, following a previous protocol [52]. Each soil sample was homogenized in 9 mL of PBS and vortexed at maximum speed (3000 rpm) for 5 min. To disaggregate soil particles and release microbial cells, the falcon conical tubes containing samples were then mildly sonicated in an ultrasonic bath (Branson Ultrasonics CPS series) for 3 min [52]. After sonication, samples were centrifuged at 2000 rpm for 15 min at 4°C to separate bacterial cells from the soil matrix. The supernatant was serially diluted in sterilized PBS and plated onto LB agar supplemented with the appropriate antibiotics and 100 nM aTc. Plates were incubated at room temperature for 40–48 h, and colonies were counted. CFU/g dry soil was calculated as described previously [53]. Soil samples were also collected after 14, 21, and 30 days to confirm the persistence or elimination of the synthetic phenol scavenger.

HPLC analysis for phenol measurement

One milliliter of microbial culture was centrifuged at 8000 rpm for 10 min at 4°C to remove cellular debris. Subsequently, 500 μL of the supernatant was collected, filtered through a 0.22 μm filter, and either analyzed immediately or stored at –80°C for later analysis. Phenol quantification was performed using an Agilent Poroshell 120 EC-C18 column (3 × 150 mm, 2.7 μm) at 25°C. Phenol peaks were detected at 254 nm using an ultraviolet spectrophotometric detector (Agilent 1100 VWD). The flow rate was maintained at 0.5 mL/min, and the mobile phase consisted of a 50:50 (v/v) mixture of acetonitrile and distilled water.

Statistical analysis

Replicates were plotted using the average, and error bars represent the standard deviation of the mean. Statistical significance was evaluated using Student's *t*-test. Regression analysis and graph plotting were conducted using GraphPad Prism v9.5 (GraphPad Software, Inc.).

Results

In this study, we aimed to develop genetic "expiry-date" circuits to ensure self-destruction of genetically engineered *E. coli*

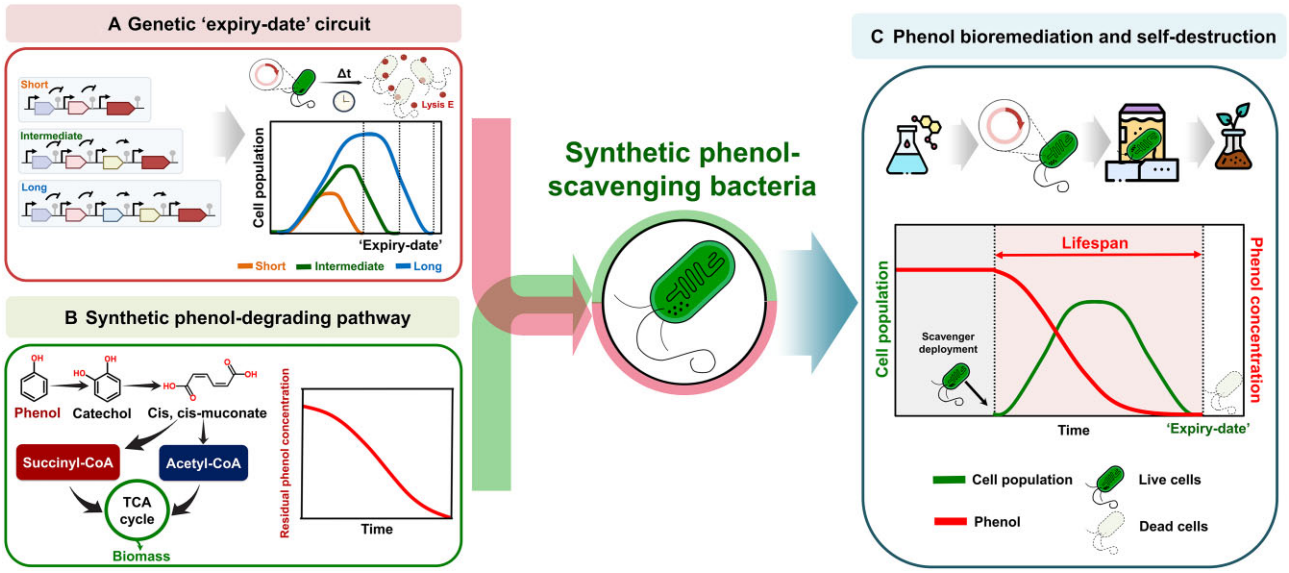

Figure 1. Development of a genetic, time-dependent self-destruction system and its application in a synthetic phenol-scavenging *E. coli*. (**A**) Genetic "expiry-date" circuits were developed to regulate the bacterial lifespan using a feedforward activation network. (**B**) In parallel, a synthetic phenol-degradation pathway was constructed to convert phenol into biomass through the TCA cycle. (**C**) When deployed, the engineered *E. coli* strain equipped with both the degradation pathway and the genetic "expiry-date" circuit successfully performed efficient phenol bioremediation, followed by autonomous self-elimination.

strain, which can detoxify phenol efficiently as a proof of concept (Fig. 1). To achieve this goal, we first designed and characterized feedforward network-based genetic "expiry-date" circuits to control the lifespan of the synthetic bacteria. Next, we constructed a synthetic phenol degradation pathway and introduced the pathway with the genetic "expiry-date" circuits into *E. coli*, creating synthetic scavenger bacteria for phenol bioremediation. Finally, we assessed both phenol degradation efficiency and programmed self-destruction of the engineered bacteria in laboratory and soil environments.

Design of feedforward network-based genetic "expiry-date" circuits and their mathematical simulation

We developed three synthetic genetic circuits that function as "expiry-date" mechanisms, designed to eliminate the host organism after a predetermined duration (Fig. 2A). These circuits utilize feedforward networks, which consist of two repressors and a variable number of activators. We integrated two consecutive repressors to eliminate the need for external inducers to trigger the feedforward cascade, ensuring autonomous operation in an open environment. The number of activators in the network determines the lifespan of the host bacteria. As illustrated in Fig. 2A, the first repressor R_1 is constitutively expressed, while the second repressor R_2 is repressed by R_1. Under permissive conditions, the inducer binds to R_1, inhibiting its repressive activity. This allows R_2 to be expressed, which in turn blocks the downstream feedforward cascade, preventing expression of the cell-killing protein K and allowing the cells to survive. In nonpermissive conditions—such as in open environments without the inducer—R_1 constitutively represses R_2 expression. As R_2 levels decline over time, the feedforward cascade (A_1 and A_2) becomes activated, ultimately triggering the production of the cell-killing protein K and leading to cell death.

The development of a mathematical model to simulate these theoretical genetic "expiry-date" circuits is detailed in Supplementary Fig. S1. Model construction and reaction parameters are provided in Supplementary Text S1 and Supplementary Table S1. To account for gene expression noise and cellular fluctuations, we stochastically simulated the models using the GillesPy2 Python library (https://pypi.org/project/gillespy2), which implements the Gillespie algorithm [54]. To replicate cell population heterogeneity, we initiated the simulation with 200 cells in varying states, such as different initial growth stages, and repeated the simulation 100 times.

Cells containing one of the three circuits—short, intermediate, or long "expiry-date"—were predicted to be eliminated in a specific order based on the time delay associated with the number of steps in the feedforward network (Fig. 2B). The average lifespans of these populations are presented in Fig. 2C. These results indicate that the designed genetic circuits can impose a predefined lifespan, making them suitable for assigning a programmed expiry date to synthetic bacteria.

To implement these genetic "expiry-date" circuits in real-world settings and simulate the realistic circuits, we used two repressors (TetR and CI), two transcriptional activators (AraC and LuxR), and Lysis E [55] for induced cell death (Fig. 2D). In cells harboring the short "expiry-date" circuit, the presence of aTc during laboratory incubation induces expression of the repressor CI, which inhibits production of the lytic protein Lysis E. In the absence of aTc—such as in an open environment—CI is naturally degraded, allowing Lysis E expression to initiate and ultimately inducing cell death. Similarly, in cells harboring the long "expiry-date" circuit, the circuit remains inactive in the presence of aTc. Upon removal of aTc, after CI degrades, the first transcription activator AraC is produced, triggering the production of the second activator LuxR. LuxR then activates Lysis E expression, leading to cell death. The distinction between the intermediate and long "expiry-date" circuits

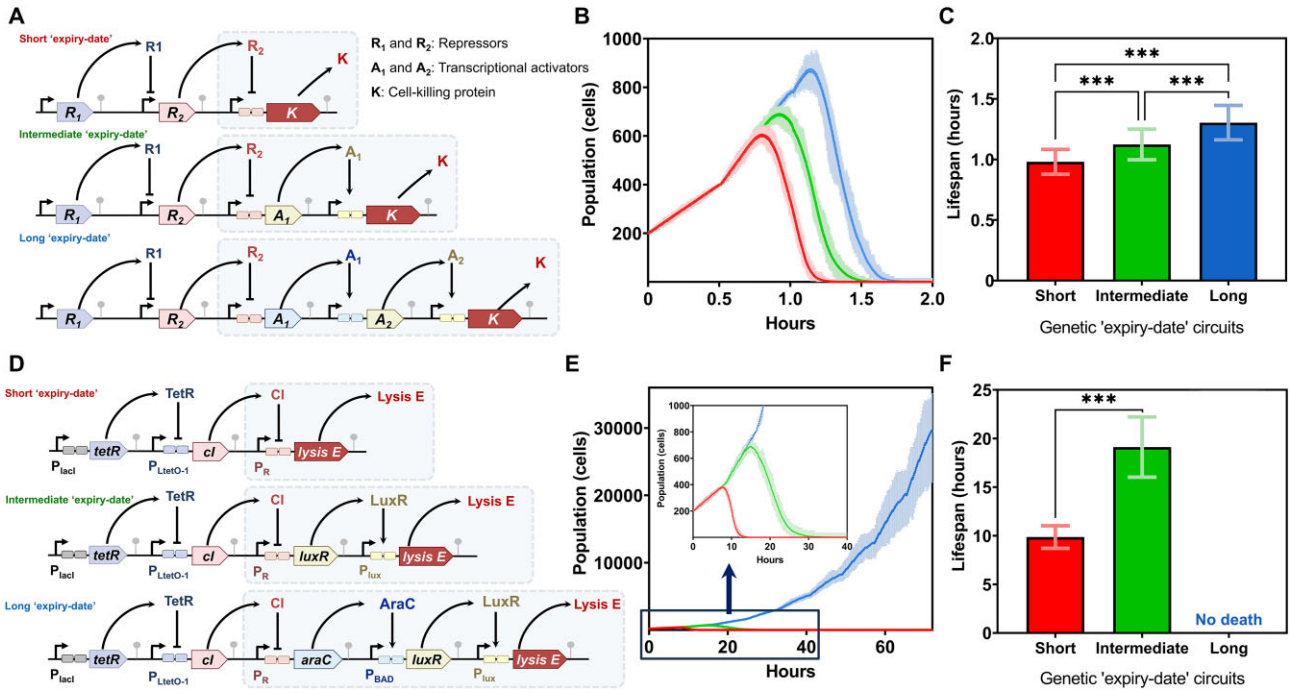

Figure 2. Schematics of genetic "expiry-date" circuits and mathematical simulation results. (**A**) Diagrams of theoretical genetic "expiry-date" circuits designed to control the lifespan of *E. coli*. The circuit architecture is a transcriptional cascade composed of two repressors (R_1 and R_2), two activators (A_1 and A_2), and a terminal cell-killing protein (K). The circuit's function is governed by a transcriptional cascade involving two repressors (R_1 and R_2), two activators (A_1 and A_2), and a terminal cell-killing protein (K). The circuit's state is determined by an external inducer. In permissive conditions, the presence of the inducer inhibits R_1, which in turn allows for the expression of R_2. This R_2 protein then suppresses the downstream cascade, preventing the production of the killing protein and ensuring cell survival. Conversely, in the absence of the inducer, an active R_1 represses R_2 expression. This de-represses the downstream cascade, leading to the sequential activation of A_1 and A_2, which ultimately triggers expression of the killing protein K and results in cell death. (**B** and **C**) Stochastic simulation results for the three theoretical genetic "expiry-date" circuits: (B) bacterial population over time and (C) average lifespan. (**D**) Diagrams of realistic genetic "expiry-date" circuits deploying the transcriptional repressors TetR and CI, activators AraC and LuxR, and the cell-killing protein Lysis E. The circuit's function is governed by the presence of aTc. In the presence of aTc, the inducer inactivates the TetR repressor, permitting the expression of CI from the $P_{LtetO-1}$ promoter. CI subsequently blocks the downstream cell-death pathway, ensuring cell survival. Conversely, in the absence of aTc, TetR actively represses CI expression. The resulting depletion of CI relieves repression of the downstream cascade, enabling sequential activation by AraC and LuxR, which ultimately induces the expression of Lysis E and triggers cell elimination. (**E** and **F**) Stochastic simulation results for the three realistic genetic "expiry-date" circuits: (E) bacterial population over time and (F) average lifespan. In (A) and (D), dashed rectangles represent the genetic components and reactions modeled for simulation (Supplementary Text S1, Supplementary Figs S1 and S2, Supplementary Tables S1 and S2). Statistical significance among circuits was determined by Student's *t*-test; asterisks indicate *P*-values: $***P < 0.001$. Error bars represent the standard deviation of the mean ($n = 20\,000$).

lies in the number of feedforward transcriptional activation steps. The short "expiry-date" provides the shortest lifespan, while the long "expiry-date" confers the longest. The modularity of this feedforward network allows precise control over the timing of Lysis E expression—and therefore the lifespan of the host organism—by adjusting the number of transcriptional steps.

To assess the functionality of the practical circuit designs, we developed additional mathematical models for the short, intermediate, and long "expiry-date" circuits (Supplementary Fig. S2). Detailed model construction and reaction parameters are provided in Supplementary Text S1 and Supplementary Table S2. The primary differences between the realistic circuits and the theoretical ones are a significantly longer doubling time (8 h), resulting in slower reaction rates [56–58], and variable promoter strengths, with strong P_R, intermediate P_{lux}, and relatively weak P_{BAD} promoters (Supplementary Text S1).

As shown in Fig. 2E, synthetic bacteria harboring the short, intermediate, or long "expiry-date" circuits were predicted to display distinct growth profiles. As expected, cells with the short circuit exhibited the earliest reduction in growth, followed by those with the intermediate circuit. The decrease in growth was attributed to the timely expression of the cell-killing protein Lysis E. Interestingly, cells with the long "expiry-date" circuit avoided cell death. This was due to insufficient production of Lysis E, resulting from the comparatively weak P_{BAD} promoter in the middle of the feedforward network. Additionally, dilution of Lysis E due to cell division further impeded its accumulation, hindering cell death. When we increased the promoter strength to a level similar to that of the P_R promoter in the mathematical simulation, the long "expiry-date" circuit successfully showed an extended growth period compared with the intermediate circuit, and the cells ultimately underwent cell death (Supplementary Fig. S3). This highlights the delicate balance between promoter strength, gene expression, and cellular processes, offering insight into potential adjustments needed for more effective circuit design.

Due to inherent gene expression variability, individual cells died at slightly different times, with some dying earlier and others later than expected. Nevertheless, the average growth profiles clearly differed among the short, intermediate, and long "expiry-date" circuits. When comparing the circuits' average lifespans—the time until death—there was a significant difference among the circuits (Fig. 2F). The predicted lifespans

for the short and intermediate circuits were 10 and 20 h, respectively. As noted, the long circuit did not induce cell death entirely, so cells with this circuit did not have a defined lifespan. Our mathematical simulations demonstrate that the designed circuits can effectively impose distinct lifespans on synthetic bacteria, providing a controlled "expiry-date" for their use in open environments. Additionally, the models can be utilized to optimize the circuits, ensuring reliable execution of programmed tasks.

Implementation of the designed genetic "expiry-date" circuits with different lifespans

To evaluate the reliability of each step in our genetic "expiry-date" circuits, we investigated mutant forms of CI, LuxR, and AraC to ensure tight inhibition and reliable triggering of the feedforward network. We first tested three variants of the CI repressor: wild-type CI, CI^{857} [43], and CI^{ts2} [59]. These variants were expressed under the control of the $P_{LtetO-1}$ promoter, and EGFP expression, driven by the P_R promoter, was measured in media with or without aTc to identify the most effective CI variant (Fig. 3A). The wild-type CI exhibited strong repression of EGFP expression regardless of the presence of aTc, indicating it would not activate the genetic circuit at all. In contrast, the mutant forms enabled EGFP production, with CI^{ts2} showing the lowest background expression and the strongest activation. Based on these results, we selected CI^{ts2} as a key component of our genetic "expiry-date" circuits.

The transcriptional activators AraC and LuxR are normally activated by their respective inducers, L-arabinose and the autoinducer 3OC6-HSL. However, reliance on these environmental inducers could interfere with the function of the genetic "expiry-date" circuits. To mitigate such interference, we tested mutant forms of these transcriptional activators that are insensitive to their inducers while retaining sufficient activity to drive the feedforward network. As shown in Fig. 3B, we evaluated three mutant forms of AraC—$AraC^{L9P}$, $AraC^{T13H}$, and $AraC^{V20M}$—based on their ability to activate the P_{BAD} promoter independently of L-arabinose. These mutants have been reported to be insensitive to L-arabinose while maintaining constitutive activation of the P_{BAD} promoter [60]. Among them, $AraC^{V20M}$ displayed the highest activity regardless of L-arabinose presence, making it the optimal choice for our feedforward network. Similarly, we evaluated LuxR mutants ($LuxR^{A221V}$ and $LuxR\Delta_{2-162}$), which have been reported to function independently of the autoinducer 3OC6-HSL, for their ability to activate the P_{lux} promoter [61]. The wild-type LuxR and $LuxR\Delta_{2-162}$ failed to activate the P_{lux} promoter in the absence of the autoinducer 3OC6-HSL, whereas $LuxR^{A221V}$ successfully activated the promoter, albeit with partial sensitivity to the inducer. Therefore, we selected $LuxR^{A221V}$ for incorporation into the genetic "expiry-date" circuits (Fig. 3C).

Besides interference from chemical inducers, leaky transcription from promoters is a major factor contributing to circuit instability [62–64]. To address this, we evaluated the basal transcription levels of the three promoters used in our circuits: P_R, P_{BAD}, and P_{lux} (Fig. 4A–C). While P_R and P_{BAD} showed minimal background activity in the absence of their respective regulators, P_{lux} exhibited significant leakiness even without the $LuxR^{A221V}$ activator (Fig. 4D). As P_{lux} promoter is employed in the intermediate and long "expiry-date" circuits to express Lysis E, this high basal transcription could lead to unintended Lysis E production (Fig. 2D), potentially disrupting the programmed function of our genetic "expiry-date" circuits.

To mitigate this issue, we incorporated sRNA to suppress the leakiness of Lysis E expression in the circuits, as described in a previous study [46]. Supplementary Figure S4 demonstrates that, in the absence of synthetic anti-*lysis E* sRNA, leaky expression of Lysis E impaired cell growth in circuits utilizing the P_{lux} promoter. In contrast, the incorporation of anti-*lysis E* sRNA effectively suppressed this leakiness and restored normal growth under permissive conditions, thereby confirming the functionality of the circuits. Interestingly, the short "expiry-date" circuit in which Lysis E is expressed under the tightly regulated P_R promoter, exhibited greater stability over time compared with intermediate and long "expiry-date" circuits. Nevertheless, the incorporation of synthetic anti-*lysis E* sRNA further improved the stability of the short "expiry-date" circuit. These results indicate that synthetic sRNA-mediated post-transcriptional repression enhances the robustness of genetic circuits by minimizing unintended gene expression. Based on these optimizations, the final designs of the genetic "expiry-date" circuits—short, intermediate, and long with varying lifespans—are presented in Fig. 5A.

Incorporation of additional kill switch for ensured self-destruction of synthetic bacteria

The genetic "expiry-date" circuit relies on a single kill switch, Lysis E. However, since the circuit is carried on a low-copy-number plasmid (pSC101 origin), there is a risk of plasmid loss during cell division, potentially allowing synthetic bacteria to evade programmed cell death. To address this, we engineered a stable *E. coli* chassis by knocking out the essential *asd* gene, rendering the strain auxotrophic [65], and then reintroducing *asd* on the plasmid carrying the genetic "expiry-date" system (Fig. 5B). The *asd* gene encodes aspartate-semialdehyde dehydrogenase, a critical enzyme in the biosynthetic pathway from aspartate to lysine [66]. DAP, a direct precursor of lysine in this pathway, is also essential for the synthesis of peptidoglycan, a key component of the bacterial cell wall. As a result, the engineered *E. coli* strain can only survive when supplemented with DAP [67, 68]. In open environments without DAP supplementation, loss of the plasmid carrying the genetic "expiry-date" system leads to cell death due to the absence of the *asd* gene. The essentiality of *asd* for bacterial survival was confirmed by monitoring the growth of the engineered chassis (Supplementary Fig. S5).

Finally, we recorded the kinetic growth curves of the *asd*-knockout chassis harboring a plasmid containing both the genetic "expiry-date" circuit and the *asd* gene (Fig. 5C–E). The death phases of cells carrying the short, intermediate, or long "expiry-date" circuits were initiated at ~1, 11, and 25 h, respectively (Fig. 5C–E). To determine the exact lifespans of these synthetic bacteria, we quantified viable cells and calculated survival ratios at 12, 24, 36, and 48 h post-culture (Fig. 5F). As shown in Fig. 5G, bacteria with the short and intermediate "expiry-date" circuits became undetectable ($<10^{-10}$)—meeting the U.S. NIH standards for GMO release ($<10^{-8}$) [69]—after 12 and 36 h, respectively. This confirms that cells with the short circuit had an effective lifespan of <12 h, while those with the intermediate circuit were eliminated within 36 h.

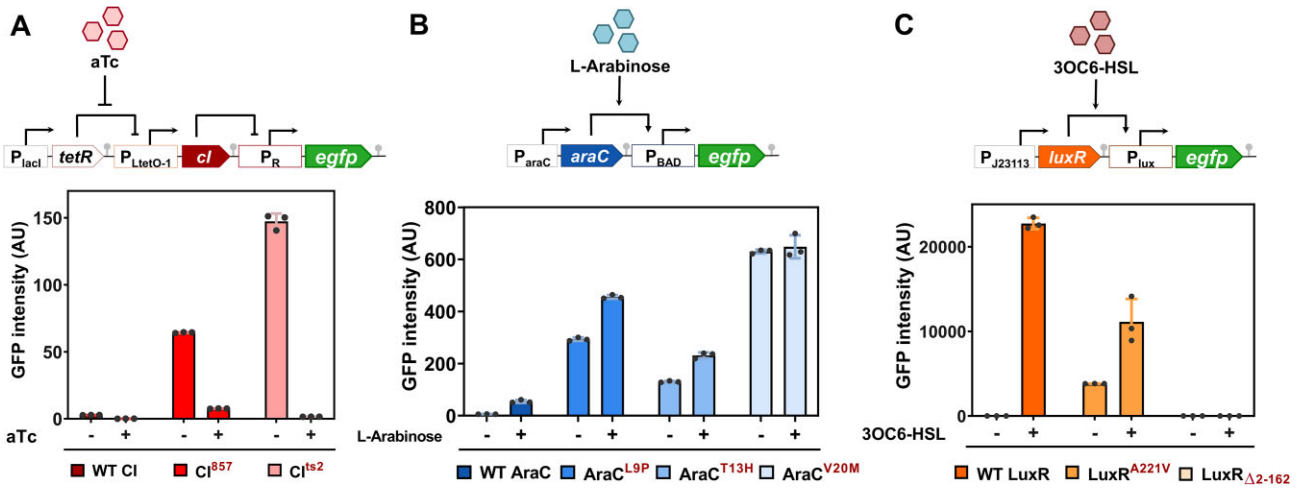

Figure 3. Transcriptional activity and inducer dependency of transcriptional regulators and their variants. (**A**) The repressive activity of CI variants on the P_R promoter was evaluated by measuring fluorescence from a P_R-driven enhanced green fluorescent protein (EGFP) reporter. The expression of each CI variant was controlled by the $P_{LtetO-1}$ promoter, and its activity was assessed in the presence and absence of 100 nM aTc. (**B**) The activation of the P_{BAD} promoter by variants of the transcriptional activator AraC was quantified by measuring the relative fluorescence of a downstream EGFP reporter. This assessment was performed with and without the addition of 0.02% L-arabinose. (**C**) Similarly, the activity of LuxR transcriptional activator variants on the P_{lux} promoter was determined by measuring EGFP fluorescence in the presence and absence of 1000 nM 3OC6-HSL. All experiments were performed in triplicate; error bars represent the standard deviation of the mean ($n = 3$).

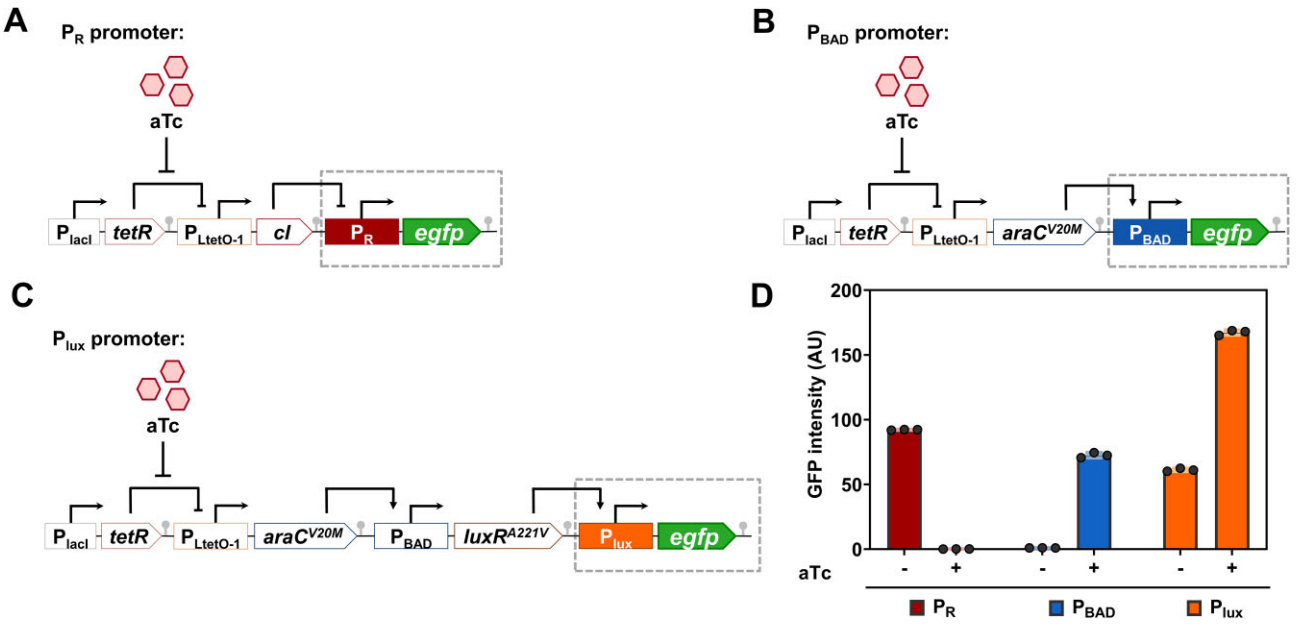

Figure 4. Evaluation of promoter leakiness in the genetic "expiry-date" circuits. (**A**–**C**) To assess promoter leakiness, EGFP reporter expression from the P_R, P_{BAD}, and P_{lux} promoters was quantified via flow cytometry. In the corresponding tests, the transcriptional regulators (CI^{ts2}, $AraC^{V20M}$, and $LuxR^{A221V}$) were expressed from the $P_{LtetO-1}$ promoter. Basal promoter activity was then measured in the presence or absence of 100 nM aTc to evaluate reporter expression under repressive conditions. (**D**) EGFP fluorescence was analyzed as described in the "Materials and methods" section. All experiments were performed in triplicate, and error bars represent the standard deviation of the mean ($n = 3$).

To confirm genetic stability and rule out escape mutants, we performed next-generation sequencing (NGS) of the whole plasmids from cells carrying the intermediate "expiry-date" circuit at 12 h post-induction, a time point at which cells are expected to experience elevated stress due to the expression of the death-inducing protein, Lysis E. However, analysis of the NGS data revealed that there were no functionally disruptive mutations within the plasmids (Supplementary Text S2 and Supplementary Table S3). To further evaluate the long-term stability of the plasmid containing the circuit, we incubated the cells for 14 days and every second day we assessed whether their circuit was still operational (Supplementary Fig. S6). At least for 14 days, the plasmid was maintained within the cells and the circuit within the plasmid was able to behave as programmed. These results demonstrate both long-term circuit stability and effective self-elimination. Consistent with our realistic simulation results, cells with the long "expiry-date" circuit did not undergo complete cell death. However, their growth was significantly slowed due to low-level production of Lysis E (Fig. 5E and G).

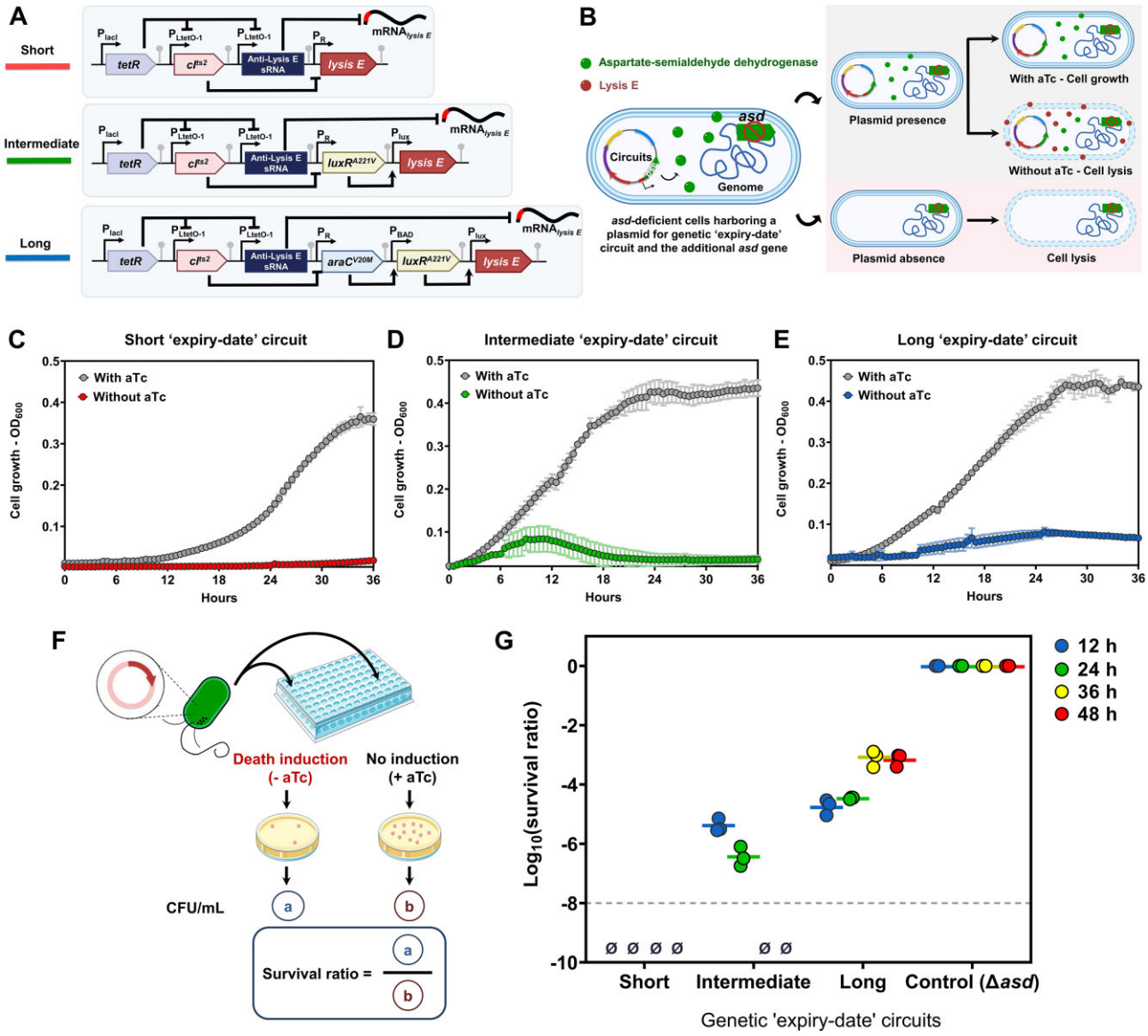

Figure 5. Implementation and evaluation of genetic "expiry-date" circuits. (**A**) Schematic diagrams of the implemented genetic "expiry-date" circuits designed for short, intermediate, and long lifespans. (**B**) The plasmid stabilization strategy, which moves the essential *asd* gene from the chromosome to the plasmid. The loss of the plasmid is lethal due to the resulting inability to synthesize peptidoglycan. (**C**–**E**) Growth curves of synthetic bacteria with each "expiry-date" circuit. Growth curves were recorded over 36 h in M9 minimal medium at 25°C. The cultures were grown with and without the inducer (aTc) to mimic permissive and non-permissive environmental conditions. (**F**) Experimental workflow for the survival assay to evaluate the circuit efficiency. (**G**) Survival ratios quantified at specified time points (12, 24, 36, and 48 h of incubation) by determining CFUs. Cell viability below the detection limit ($<1 \times 10^{-10}$) is indicated by the symbol "Ø." All experiments were performed in triplicate and error bars represent the standard deviation of the mean ($n = 3$).

Motivated by our mathematical model's prediction that the weak P_{BAD} promoter impaired the expected behavior of the original design (Fig. 2E and F, and Supplementary Fig. S3), we substituted the AraC–P_{BAD} pair in the long "expiry-date" circuit with the T7 promoter and its cognate T7 RNA polymerase, aiming to enhance circuit robustness. Given that the T7 promoter is reported to be 5–50 times stronger than the P_R promoter [70–73], we simulated the revised long "expiry-date" circuit using T7 promoter strengths across this range. As shown in Supplementary Fig. S7, the simulations predicted that the circuit would paradoxically exhibit a lifespan equal to or shorter than that of the intermediate circuit, due to excessive promoter strength causing premature activation (Supplementary Fig. S7). To confirm this, we experimentally constructed and tested the revised circuit. Unlike our simulations, cells harboring this circuit exhibited no detectable growth from the outset (Supplementary Fig. S8). This is consistent with previous reports indicating that overexpression of T7 RNA polymerase consumes a disproportionate share of cellular resources and may deplete essential host nutrients, ultimately leading to significant growth inhibition [74–76]. In our nutrient-limited conditions, this burden appeared to be exacerbated, resulting in circuit failure and lack of growth. Consequently, the construction of a robust long "expiry-date" circuit will require transcriptional activators that are sufficiently strong—comparable to the P_R promoter—function independently of chemical inducers or repressors, and are fully compatible with *E. coli*, which at present remains a signif-

icant challenge. Given these constraints, we prioritized the short and intermediate "expiry-date" circuits to confer a predetermined lifespan to synthetic bacteria developed for phenol scavenging.

Selection of a phenol-tolerant *E. coli* strain and further tolerance improvement

As a practical application of our "expiry-date" circuit, we employed the intermediate circuit to regulate the lifespan of phenol-degrading synthetic bacteria for safe bioremediation. Phenol is a hazardous pollutant and poses a significant environmental challenge due to its widespread use and persistence [35]. Its high toxicity to living organisms, including *E. coli*, limits the effectiveness of microbial bioremediation efforts. Therefore, the initial step in developing a synthetic scavenger involves selecting an *E. coli* strain with higher inherent phenol tolerance and then enhancing its tolerance further.

Different *E. coli* strains exhibit a wide range of physiological characteristics that significantly influence their ability to tolerate high concentrations of phenol. In a previous study, 18 different *E. coli* strains were evaluated for their ability to tolerate phenol, and the BL21 (DE3) strain exhibited the greatest phenol resistance [77]. This strain was able to survive in medium containing 1.6 g/L of phenol, while complete growth inhibition occurred at 1.8 g/L. To identify more tolerant *E. coli* strains, we evaluated additional strains for phenol tolerance that had not been tested before: MK01 derived from K-12 BW27783, SURE from K-12, JM109 from K-12, LS5218 from K-12, and BL21 (DE3) from the B strain as a reference (Supplementary Table S4).

The growth of *E. coli* strains was monitored for 24 h under various phenol concentrations (Supplementary Fig. S9). As phenol concentration increased, growth slowed and was eventually inhibited. In the phenol range of 0–1.5 g/L, the MK01 strain exhibited significantly higher growth, with the largest growth difference observed at 1.0 g/L phenol (Supplementary Fig. S9D). Up to 1.5 g/L phenol, MK01 showed significantly higher phenol tolerance than other tested strains (Supplementary Fig. S9E). At 2.0 g/L phenol, the growth of most strains was inhibited: complete growth inhibition was observed for both SURE and BL21 (DE3) strains, while LS5218 and MK01 showed slight growth (Supplementary Fig. S9F). Phenol tolerance, calculated using Equation (2), demonstrated that MK01 had significantly higher tolerance and growth rates than BL21 (DE3) (Fig. 6A and B), which had previously been identified as the most phenol-tolerant *E. coli* strain [77]. Based on these results, the MK01 strain was selected as the chassis for developing a synthetic scavenger for phenol degradation and the implementation of a programmed lifespan.

To further enhance the phenol tolerance of the MK01 strain, we expressed two mutant proteins, $SecB^{T10A}$ [78] and $RpoD^{C9}$ (D39E, A72V, T94M, and a nonsense mutation at residue 123) [79], either individually or in combination, using three different synthetic promoters with varying strengths (high, medium, and low) (Fig. 6C). These mutants were chosen because they have been shown to enhance tolerance to butanol and other organic solvents in *E. coli* [78, 79]. SecB is a chaperone involved in translocating proteins across the inner membrane, integrating proteins into the membrane, and aiding protein folding in the cytoplasm [80]. Its role in stress response and protein stability could support *E. coli* tolerance to phenol by maintaining proper protein folding and membrane integrity under stress [81, 82]. The $SecB^{T10A}$ mutant was selected for its improved chaperone activity [78, 83]. RpoD (σ^{70}) is the primary sigma factor in *E. coli*, essential for regulating the expression of genes during the exponential phase [84]. It plays a key role in the cellular response to stress and solvent tolerance by modulating gene expression to cope with harmful compounds [85, 86]. The $RpoD^{C9}$ mutant was chosen for its ability to regulate stress response pathways more effectively, improving the cells' adaptation to phenol exposure [79].

Nine plasmids were constructed to express these mutant genes under the three different promoters (Fig. 6C). These plasmids were introduced into the MK01 strain, and phenol tolerance was evaluated at concentrations ranging from 0 to 2.0 g/L over 24 h. As shown in Fig. 6D, the additional expression of either $RpoD^{C9}$ or $SecB^{T10A}$ could enhance phenol tolerance, but cells expressing $RpoD^{C9}$ displayed significantly higher tolerance than those expressing either $SecB^{T10A}$ alone or both genes together, irrespective of promoter strength. Notably, cells expressing $RpoD^{C9}$ under a weak promoter (J23113) exhibited slightly better tolerance than those using stronger promoters at high phenol concentrations. Interestingly, co-expression of both mutant genes resulted in lower tolerance compared with cells expressing either gene individually (Fig. 6D). Furthermore, in the absence of phenol, co-expressing cells displayed a noticeably slower growth rate (Fig. 6E, symbols below the control cells, black dotted line). Given that SecB and RpoD are global regulators involved in various cellular processes, their co-expression may impose a metabolic burden on the host cells, thus affecting overall growth and tolerance.

These findings suggest that optimized expression of the $RpoD^{C9}$ mutant significantly enhances phenol tolerance. Consequently, the $RpoD^{C9}$ mutant expressed by the weak promoter (J23113) was incorporated into the MK01 synthetic bacteria chassis to further improve phenol degradation and tolerance.

Construction of a synthetic metabolic pathway converting phenol to acetyl-CoA

To enable the degradation and utilization of phenol as an energy source, we constructed a synthetic metabolic pathway consisting of nine genes that convert phenol into succinyl-CoA and acetyl-CoA, key intermediates in the tricarboxylic acid (TCA) cycle (Fig. 7A) [87, 88]. This catechol ortho-cleavage pathway enables engineered bacteria to metabolize phenol as a carbon source for biomass production [89]. To construct the pathway, we expressed the *phe* operon derived from *R. erythropolis* KCTC 3483 and the *pca* and *cat* operons from *P. putida* KT2440 (Fig. 7A). Detailed information on the genes encoding the enzymes for this pathway is provided in Supplementary Table S5. The nine genes were cloned into two plasmids and expressed under the control of a strong synthetic promoter (J23119) in a polycistronic arrangement (Fig. 7B). The J23119 promoter, comparable in strength to the widely used T7 promoter, is known for its efficiency in recombinant protein overexpression [90]. To further enhance phenol tolerance, the J23113-$rpoD^{C9}$ gene was also incorporated into one of the plasmids (Fig. 7B and Supplementary Fig. S10).

The performance of the engineered synthetic phenol scavenger was assessed by measuring its efficiency in degrading phenol at varying initial concentrations, ranging from

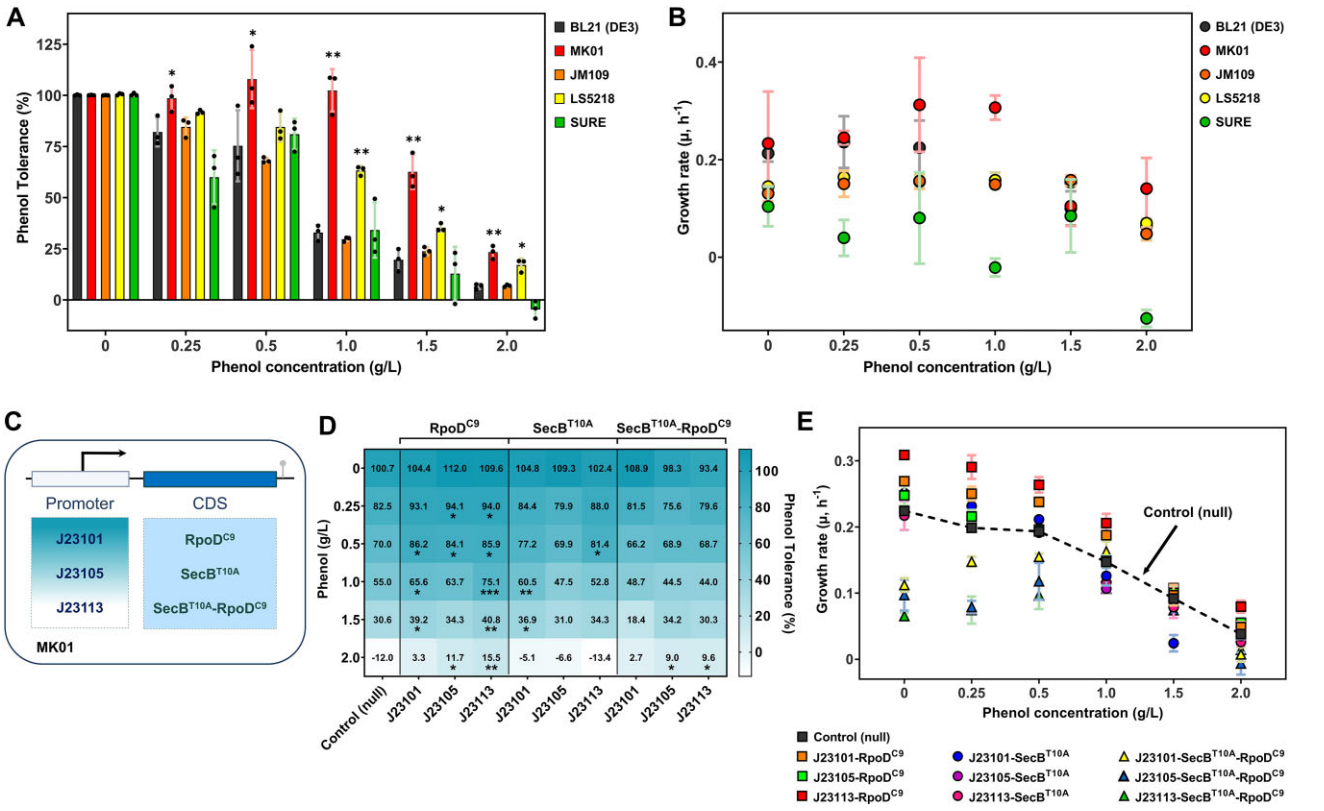

Figure 6. Development of an *E. coli* chassis with enhanced phenol tolerance. (**A**) Phenol tolerance of five *E. coli* strains cultured in LB medium supplemented with increasing concentrations of phenol. (**B**) Corresponding growth rates of these strains under phenol stress conditions. (**C**) Gene constructs designed to express the chaperone mutant $SecB^{T10A}$, the sigma factor mutant $RpoD^{C9}$, or both, using a series of synthetic promoters with varying strengths (J23101 (strong), J23105 (medium), and J23113 (weak)) to enhance phenol tolerance of *E. coli* MK01. (**D**) Phenol tolerance of *E. coli* MK01 strains engineered to express individual or combined tolerance-enhancing proteins. The tolerance of these strains was quantified across a range of phenol concentrations according to the formula presented in Equation (2). (**E**) Growth rates of the engineered strains during phenol tolerance experiments. Statistical significance was assessed using Student's *t*-test; asterisks represent *P*-values (*$P < 0.05$, **$P < 0.01$, ***$P < 0.001$). All experiments were performed in triplicate; error bars represent the standard deviation of the mean ($n = 3$).

0.1 to 1.5 g/L (Fig. 7C). The synthetic bacteria exhibited significantly improved phenol degradation capabilities compared with previously developed strains (Table 1) [36, 39, 40, 87, 91–96]. Specifically, the synthetic bacteria completely degraded 0.1 g/L of phenol within 2 h and 0.3 g/L within 7 h. For 0.5 g/L of phenol, detoxification was achieved within 48 h. Although complete removal of phenol at higher concentrations (1.0 and 1.5 g/L) was not achieved within 48 h, the bacteria steadily reduced the phenol concentration over time (Fig. 7C). Interestingly, despite the cellular burden imposed by the additional expression of the synthetic metabolic pathway—which slows the growth of the synthetic bacteria—their growth was unaffected by phenol concentrations up to 1.5 g/L (Supplementary Figs S10B and S11). This high phenol tolerance is likely the result of a synergistic effect between the enhanced tolerance conferred by $RpoD^{C9}$ and the phenol degradation capability provided by the synthetic metabolic pathway.

Construction of synthetic phenol scavenger bacteria with an "expiry-date"

To construct synthetic phenol-scavenging bacteria capable of safe bioremediation, we introduced plasmids containing the engineered synthetic phenol degradation pathway into an *E. coli* chassis with a predetermined "expiry-date" (*E. coli* MK01Δ*asd* strain carrying a genetic "expiry-date" circuit) (Fig. 8A). The bioremediation performance of the synthetic bacteria was first evaluated at initial phenol concentrations of 0.1, 0.3, and 0.5 g/L (Fig. 8B). As a control, we used the *E. coli* MK01Δ*asd* strain containing only the phenol degradation pathway, without the "expiry-date" circuit, since it does not undergo programmed cell death.

The control strain achieved complete degradation of 0.1, 0.3, and 0.5 g/L phenol within 2, 7, and 12 h, respectively, surpassing previously reported performance (Fig. 8B and Table 1). In contrast, the synthetic bacteria with the short "expiry-date" circuit degraded only 0.05 g/L phenol over 48 h at all initial concentrations and did not achieve complete degradation within its designated lifespan. Synthetic bacteria with the intermediate "expiry-date" circuit fully degraded 0.1 g/L phenol within 14 h but failed to completely remove phenol at initial concentrations of 0.3 and 0.5 g/L.

The inability of the synthetic scavengers to fully degrade phenol at higher concentrations is attributed to their limited lifespan. Although the synthetic scavengers with the short and intermediate "expiry-date" circuits have lifespans of 12 and 36 h, respectively, they entered the death phase earlier (at 1 and 11 h, respectively) and were unable to proliferate sufficiently for complete phenol removal. This limitation could be addressed by periodic deployment of synthetic scavenger bacteria or by developing an "expiry-date" circuit with an ex-

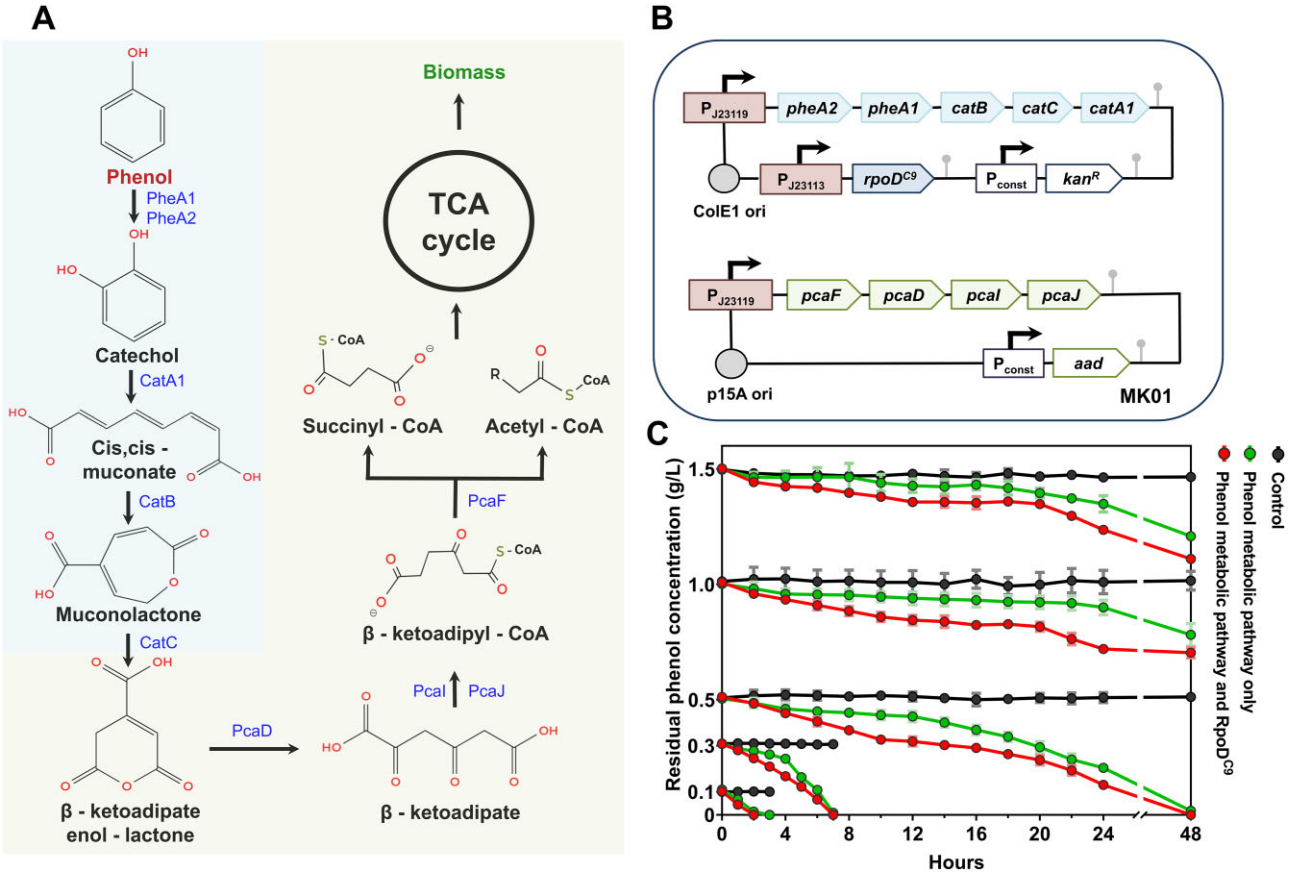

Figure 7. Construction and evaluation of a synthetic phenol-degrading metabolic pathway. (**A**) Schematic of the synthetic pathway engineered to convert phenol to β-ketoadipate, which is subsequently metabolized into the TCA cycle intermediates (succinyl-CoA and acetyl-CoA). (**B**) Plasmid constructs encoding the synthetic phenol-degrading pathway and the *rpoD*^{C9} gene. The pathway comprises nine catabolic enzymes (*pheA1*, *pheA2*, *catA1*, *catB*, *catC*, *pcaF*, *pcaD*, *pcaI*, and *pcaJ*) cloned into two separate plasmids. (**C**) Phenol degradation efficiency of the synthetic scavenger bacteria harboring the phenol metabolic pathway, with and without the *rpoD*^{C9} gene, assessed at phenol concentrations of 0.1, 0.3, 0.5, 1.0, and 1.5 g/L over 48 h. Complete degradation times were 2 h (0.1 g/L), 7 h (0.3 g/L), and 48 h (0.5 g/L); values for 1.0 and 1.5 g/L were extrapolated (see "Materials and methods" section). All experiments were performed in triplicate; error bars represent the standard deviation of the mean ($n = 3$).

Table 1. Reported phenol degradation efficiencies of various microorganisms

Bacterial strains	Strategies	Efficiency of phenol degradation	References
E. coli strain MK01Δ*asd*	Synthetic metabolic pathway construction with tolerance enhancement and "expiry-date" circuit	0.1 g/L (2 h), 0.3 g/L (7 h), 0.5 g/L (12 h)	This study
E. coli strain RV412_A1_A1_2010_06a LBK	Growth parameter optimization	0.562 g/L (230 h), 0.963 g/L (250 h)	[39]
E. coli strain BL21 (DE3)	Heterologous overexpression of enzymes	0.0941 g/L (3 h)	[87]
E. coli strain BL21 (DE3)-groELS	Genetically engineered to express diguanylate cyclases (DGCs) to promote proteinaceous and aliphatic biofloc formation	0.07 g/L (4 h)	[91]
Pseudomonas oleovorans strain ICTN13	Cells were encapsulated into the alginate matrix and tagged orange fluorescence protein gene (*ofp*) helped improving phenol degradation and tracking the survival of cells	0.09 g/L (432 h)	[92]
P. putida strain LY1	Wild-type, growth kinetic parameters optimization	0.2 g/L (40 h), 0.3 g/L (60 h)	[93]
P. putida strain KT2440	Wild-type, aromatics degradation coupled with biopolymers synthesis	0.565 g/L (144 h), 0.941 g/L (120 h)	[94]
Pseudomonas sp. strain SAS26	Novel salt-tolerant phenol-degrading bacterial strains	0.5 g/L (36 h), 1 g/L (48 h), 1.5 g/L (60 h)	[95]
R. opacus PD630 strains evol33 and evol40	Adaptive evolution	1.2 g/L (60 h)	[96]
Stenotrophomonas sp. strain N5 and *Advenella* sp. strain B9	Optimization of co-culture inoculation ratio	0.05 g/L (15 h), 0.3 g/L (30 h), 1 g/L (50 h)	[40]
Isochrysis galbana strain MACC/H59	Natural marine microalgae	<0.1 g/L (96 h)	[36]

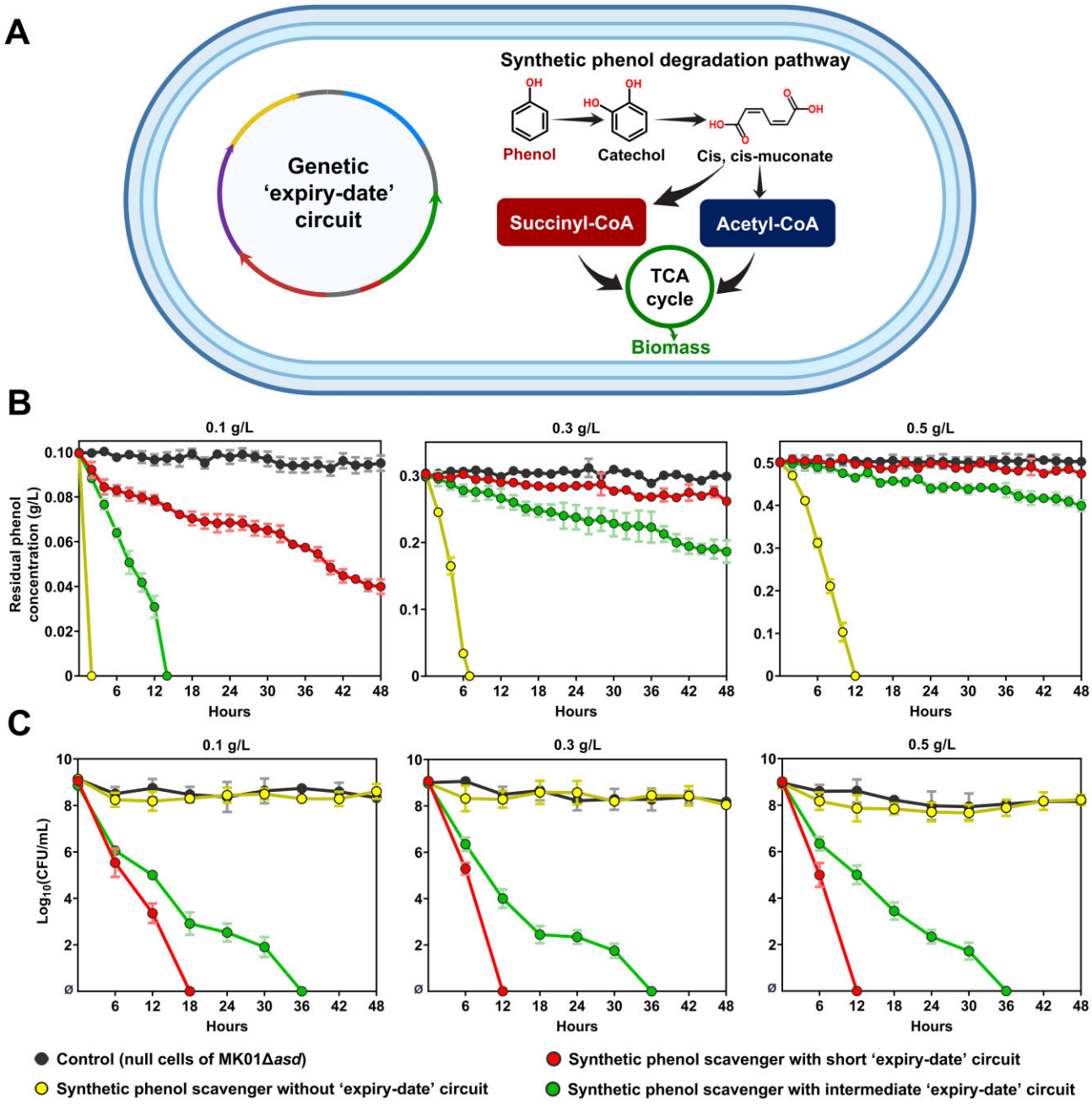

Figure 8. *In vivo* evaluation of phenol degradation efficiency and lifespan of synthetic scavenger bacteria. (**A**) Synthetic phenol scavengers were developed by introducing the plasmids encoding phenol degradation pathway into *E. coli* MK01Δ*asd* cells harboring a genetic "expiry-date" circuit. This system enables the conversion of phenol into TCA cycle intermediates for biomass production, while enabling programmed self-elimination. (**B**) Residual phenol concentrations were monitored over time at initial concentrations of 0.1, 0.3, and 0.5 g/L. The degradation performance of synthetic scavengers equipped with short or intermediate "expiry-date" circuits was compared with that of control strains and scavengers lacking the circuit. (**C**) Viable counts of synthetic scavengers (CFU/mL) were tracked to evaluate lifespan control conferred by the genetic circuits. Complete elimination of the population is indicated by "Ø" (no detectable colonies). All experiments were performed in triplicate and error bars represent the standard deviation of the mean ($n = 3$).

tended lifespan sufficient to fully degrade high concentrations of phenol.

To verify whether the synthetic scavenger bacteria underwent programmed cell death, we measured viable cell counts over time (Fig. 8C). Synthetic scavenger bacteria with the short "expiry-date" circuit showed significant declines, becoming undetectable after 18 h at 0.1 g/L phenol and after 12 h at 0.3 and 0.5 g/L phenol. Those with the intermediate "expiry-date" circuit were completely eliminated by 36 h across all phenol concentrations. Although the addition of the synthetic metabolic pathway could potentially affect cellular physiology, the observed lifespan of the synthetic scavenger bacteria closely matched that determined for bacteria with only the genetic "expiry-date" circuits (Fig. 5), indicating that the "expiry-date" circuit functions reliably and stably.

Interestingly, phenol concentration continued to decrease even after the "expiry-date," when there were no viable synthetic bacteria remaining (Fig. 8B and C). For instance, at

the initial concentration of 0.1 g/L, phenol concentration decreased over 48 h, despite the lifespan of synthetic scavenger bacteria with the short "expiry-date" circuit being only <18 h. A plausible explanation for this observation is that cell lysis induced by the cell-killing protein Lysis E released internal metabolic enzymes into the medium, allowing these enzymes to degrade phenol even after cell death. There was no evaporative loss of phenol during the experiments, as the phenol concentration in the controls remained constant over time.

Deployment of synthetic phenol scavenger bacteria in phenol-contaminated soil samples

To validate the proof of concept that synthetic scavenger bacteria can detoxify phenol in soil and subsequently self-eliminate via the genetic "expiry-date" circuit, we deployed synthetic phenol-scavenging bacteria equipped with the intermediate "expiry-date" circuit for *ex situ* testing in soil samples contaminated with phenol at 0.1 g/kg soil, a concentration corresponding to moderate contamination levels typically observed in natural soil or groundwater [48] (Fig. 9A). Residual phenol concentrations and viable cell counts of the synthetic scavenger were measured at various time points as shown in Fig. 9B and Fig. 9C. In soil inoculated with synthetic scavenger bacteria with an intermediate lifespan, phenol at an initial concentration of 0.1 g/kg of dry soil was fully degraded within 4 days (Fig. 9B). Notably, the *ex situ* soil experiments confirmed that the engineered bacteria operate effectively without supplemental carbon. The available endogenous carbon, including phenol itself, was sufficient to power both pollutant degradation and the "expiry-date" circuit. This suggests that synthetic bacterial scavengers equipped with our "expiry-date" circuit are promising candidates for a range of bioremediation purposes.

The initial count of deployed synthetic scavenger bacteria was 10^7 CFUs per gram of dry soil, and their population decreased to 10^4 and 10^3 CFUs per gram of dry soil after 3 and 4 days, respectively, becoming undetectable after 5 days (Fig. 9C and D). To confirm complete elimination of the synthetic scavengers, viable cells were monitored over the course of one month, but no detectable cells were found (Fig. 9E and F). These results confirm that the synthetic scavenger bacteria designed for phenol bioremediation can effectively detoxify contaminated soil and self-eliminate after completing their task.

Discussion

Our study highlights the potential of synthetic biology in bioremediation by engineering *E. coli* with programmed lifespans and enhanced phenol degradation capabilities. The implementation of feedforward network-based genetic "expiry-date" circuits provides a robust strategy for controlling bacterial lifespan, directly addressing biosafety concerns related to the unintended persistence and spread of synthetic bacteria in open environments.

Several biocontainment strategies have been implemented to prevent the unintended proliferation of synthetic bacteria [16, 22, 23, 28, 97]. Previous studies have utilized genetic circuits to regulate the expression of essential genes or toxin genes under defined conditions, with notable examples including CRISPR–Cas9 kill switches [23] and synthetic auxotrophic strains [98]. However, these pioneering methods often require human intervention and external stimuli, such as chemical or physical inducers, to trigger cell death [23, 97]. Furthermore, issues in genetic circuits like leaky expression of the genes in circuits have led to spurious circuit activation and thereby reduced circuit reliability [28, 97, 99].

In contrast, the genetic "expiry-date" circuit developed in this study autonomously governs cellular lifespan through an internal transcriptional cascade that initiates immediately upon deployment, without reliance on external inducers (Fig. 2D). Moreover, circuit stability is reinforced by minimizing expression leakiness through sRNA-mediated tight regulation (Supplementary Fig. S4 and Fig. 5A). These advancements collectively enable our genetic "expiry-date" system to provide stable and tunable control of bacterial lifespan.

The synthetic phenol scavenger, equipped with a genetic "expiry-date" circuit, successfully demonstrated efficient phenol degradation and programmed self-elimination (Fig. 8). Its successful application in soil environments further confirms the robustness and applicability of the "expiry-date" circuits in real-world settings (Fig. 9).

While natural phenol-degrading bacteria, such as *P. putida* [100], *P. putida* LY1 [93], and *R. opacus* PD630 [101], are known for their high intrinsic tolerance to phenol, they often degrade it at a slow rate. In contrast, *E. coli* typically exhibits lower innate tolerance to phenol, but its compatibility with a wide range of synthetic biology tools enables it to be engineered for more rapid phenol degradation than naturally tolerant strains. In this study, we further demonstrate that *E. coli*'s inherent tolerance can be enhanced: the MK01 strain, previously uncharacterized for this trait, exhibited greater phenol tolerance compared with other *E. coli* strains, and this tolerance was further improved through the expression of the $RpoD^{C9}$ (Fig. 6). These results underscore the potential of our engineered *E. coli* as a robust platform for phenol bioremediation. Furthermore, the modular "expiry-date" circuits developed in this study provide a broadly applicable biocontainment strategy that can be integrated not only into *E. coli* but also adapted for use in naturally tolerant hosts, offering a versatile and safe approach for environmental deployment.

Despite these promising results, several challenges remain for future studies. First, in this study, sterilized soil samples, artificially contaminated with phenol, were used for *ex situ* experiment due to the complexity and variability of soil conditions. Though this sterilization-and-contamination approach has been widely used [49, 102], sterilization removes natural microbial communities, preventing potential interactions between indigenous soil bacteria and the engineered strain, which could influence circuit functionality. Due to the complexity of experimental evaluation, such interactions were not assessed in this study.

Moreover, while effective, our genetic "expiry-date" system requires further optimization for broader applications. The current limitations in extending circuit lifespan highlight the need for stronger transcriptional activators balanced with precise control to enhance the longevity and adaptability of synthetic bacteria (Fig. 2, and Supplementary Figs S3 and S7). Although there are several strong repression-based transcription systems, they depend on external inducers such as isopropyl-β-D-thiogalactoside (IPTG), restricting their use in autonomous, field-deployable bioremediation contexts [103]. Other activation-based systems, such as the T7 expression platform, impose significant cellular burden

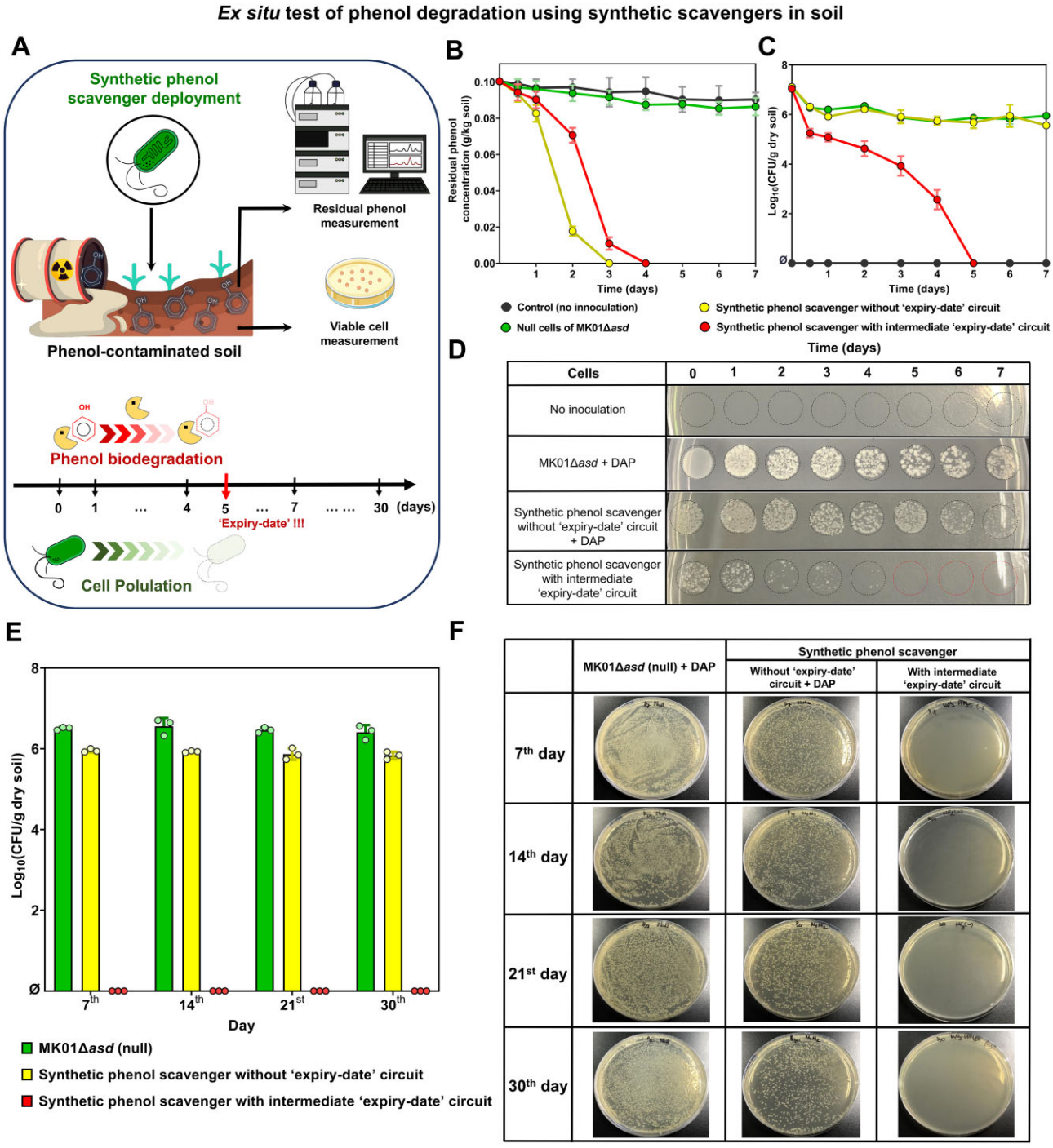

Figure 9. *Ex situ* evaluation of phenol degradation and lifespan control of synthetic scavenger bacteria. (**A**) Schematic overview of *ex situ* bioremediation setup, wherein synthetic phenol scavenger strains were introduced into phenol-contaminated soil. Residual phenol concentrations and viable cell counts were monitored over time to assess degradation efficiency and bacterial persistence. (**B**) Temporal profiles of residual phenol concentration over a 7-day period following deployment of synthetic scavengers either harboring the intermediate "expiry-date" circuit or lacking the circuit. (**C**) Viable counts (CFU/g dry soil) of synthetic scavengers monitored over time to evaluate the effectiveness of the "expiry-date" circuit in controlling bacterial lifespan. (**D**) Spot assays of soil samples collected at various time points during *ex situ* experiments, providing a visual confirmation of synthetic scavenger elimination. (**E**) Quantitative assessment of viable cell population on days 7, 14, 21, and 30 post-inoculations. The symbol "Ø" denotes that no viable colonies were detected in the samples. (**F**) Representative agar plate images showing colony formation from soil samples across time points. All experiments were performed in triplicate and error bars represent the standard deviation of the mean ($n = 3$).

[75, 76, 104], leading to circuit instability and poor performance (Supplementary Fig. S8). The limited availability and inconsistent activity of existing transcriptional activators pose a challenge [29]. In this context, CRISPR-based activators may offer an alternative solution, providing modular, precise, and time-specific control of synthetic circuits, thereby expanding the applicability of our synthetic bacteria [105].

Beyond Lysis E, additional biocontainment mechanisms should be explored to prevent unintended escape and minimize the spread of genetic material in natural environments [16]. Potential strategies include toxin–antitoxin system [106] and quadruplet codon decoding-based translation [107] to prevent unintended escape, and CRISPR–Cas9-mediated DNA disruption [27] to minimize genetic material transfer. Therefore, future work will focus on genomic integration of "expiry-date" circuits or their combination with DNA degradation mechanisms to ensure safer and more reliable synthetic microbial applications in open environments.

In conclusion, reliable genetic "expiry-date" circuits offer an effective tool for precisely controlling the lifespan of synthetic bacteria. Combined with mathematical modeling, strain optimization, and field validation, this approach provides a sustainable and scalable solution for addressing complex environmental challenges, opening new avenues for safe *in situ* bioremediation of hazardous pollutants. Furthermore, these circuits could be applied to therapeutic bacteria to mitigate the risk of uncontrolled proliferation. Our synthetic "expiry-date" circuits thus hold great promise for the responsible and effective deployment of synthetic bacteria in real-world applications.

Acknowledgements

Author contributions: Kha Mong Tran (Conceptualization [lead], Data curation [lead], Formal Analysis [lead], Investigation [lead], Methodology [lead], Validation [lead], Writing—original draft [lead]), Nuong Thi Nong (Data curation [supporting], Investigation [supporting]), Jun Ren (Data curation [supporting], Investigation [supporting]), Kangseok Lee (Data curation [supporting], Investigation [supporting]), Doheon Lee (Data curation [supporting], Investigation [supporting]), Jörg Gsponer (Investigation [supporting], Methodology [supporting], Software [lead]), Hyang-Mi Lee (Conceptualization [lead], Project administration [equal], Writing—review & editing [equal]), Dokyun Na (Conceptualization [lead], Funding acquisition [lead], Investigation [lead], Project administration [lead], Resources [lead], Software [lead], Supervision [lead], Validation [lead], Writing—original draft [lead], Writing—review & editing [lead]).

Supplementary data

Supplementary data is available at NAR online.

Conflict of interest

The authors declare no competing interests.

Funding

This work was supported by the National Research Foundation of Korea (NRF) grant funded by the Korea government (MSIT) (2022M3A9B6082687, 2023R1A2C1008156, and RS-2025-02303886). Funding to pay the Open Access publication charges for this article was provided by the NRF.

Data availability

All data supporting this study are presented in the main text and Supplementary Information. Codes for simulating the mathematical models will be shared on reasonable request to the corresponding author.

References

1. Bartoli V, Meaker GA, di Bernardo M *et al.* Tunable genetic devices through simultaneous control of transcription and translation. *Nat Commun* 2020;**11**:2095. https://doi.org/10.1038/s41467-020-15653-7
2. Hiscock TW. Adapting machine-learning algorithms to design gene circuits. *BMC Bioinf* 2019;**20**:214. https://doi.org/10.1186/s12859-019-2788-3
3. Daniel R, Rubens JR, Sarpeshkar R *et al.* Synthetic analog computation in living cells. *Nature* 2013;**497**:619–23. https://doi.org/10.1038/nature12148
4. Nguyen DH, Chong A, Hong Y *et al.* Bioengineering of bacteria for cancer immunotherapy. *Nat Commun* 2023;**14**:3553. https://doi.org/10.1038/s41467-023-39224-8
5. Shuwen H, Yifei S, Xinyue W *et al.* Advances in bacteria-based drug delivery systems for anti-tumor therapy. *Clin Trans Imm* 2024;**13**:e1518. https://doi.org/10.1002/cti2.1518
6. Yan X, Liu X, Zhao C *et al.* Applications of synthetic biology in medical and pharmaceutical fields. *Sig Transduct Target Ther* 2023;**8**:199. https://doi.org/10.1038/s41392-023-01440-5
7. Moradali MF, Rehm BHA. Bacterial biopolymers: from pathogenesis to advanced materials. *Nat Rev Micro* 2020;**18**:195–210. https://doi.org/10.1038/s41579-019-0313-3
8. Tran KM, Lee HM, Thai TD *et al.* Synthetically engineered microbial scavengers for enhanced bioremediation. *J Hazard Mater* 2021;**419**:126516. https://doi.org/10.1016/j.jhazmat.2021.126516
9. Thai TD, Lim W, Na D. Synthetic bacteria for the detection and bioremediation of heavy metals. *Front Bioeng Biotechnol* 2023;**11**:1178680. https://doi.org/10.3389/fbioe.2023.1178680
10. Chien T, Harimoto T, Kepecs B *et al.* Enhancing the tropism of bacteria via genetically programmed biosensors. *Nat Biomed Eng* 2022;**6**:94–104. https://doi.org/10.1038/s41551-021-00772-3
11. Graham AJ, Partipilo G, Dundas CM *et al.* Transcriptional regulation of living materials via extracellular electron transfer. *Nat Chem Biol* 2024;**20**:1329–40. https://doi.org/10.1038/s41589-024-01628-y
12. Zhou S. Bacteria synchronized for drug delivery. *Nature* 2016;**536**:33–4. https://doi.org/10.1038/nature18915
13. Alexander LM, van Pijkeren J-P. Modes of therapeutic delivery in synthetic microbiology. *Trends Microbiol* 2023;**31**:197–211. https://doi.org/10.1016/j.tim.2022.09.003
14. Shams A, Fischer A, Bodnar A *et al.* Perspectives on genetically engineered microorganisms and their regulation in the United States. *ACS Synth Biol* 2024;**13**:1412–23. https://doi.org/10.1021/acssynbio.4c00048
15. Yang L, Hung LY, Zhu Y *et al.* Material engineering in gut microbiome and human health. *Research* 2022;**2022**:9804014. https://doi.org/10.34133/2022/9804014
16. George DR, Danciu M, Davenport PW *et al.* A bumpy road ahead for genetic biocontainment. *Nat Commun* 2024;**15**:650. https://doi.org/10.1038/s41467-023-44531-1
17. Lee JW, Chan CTY, Slomovic S *et al.* Next-generation biocontainment systems for engineered organisms. *Nat Chem Biol* 2018;**14**:530–7. https://doi.org/10.1038/s41589-018-0056-x

18. Moon TS. SynMADE: synthetic microbiota across diverse ecosystems. *Trends Biotechnol* 2022;**40**:1405–14. https://doi.org/10.1016/j.tibtech.2022.08.010
19. Wang Y, Qian C, Deng Y-D *et al.* Development of "environmentally friendly" super *Escherichia coli* strains that can completely biodegrade toluene. *Chem Eng J* 2025;**506**:159877. https://doi.org/10.1016/j.cej.2025.159877
20. Ivanov V, Stabnikov V, Stabnikova O *et al.* Environmental safety and biosafety in construction biotechnology. *World J Microbiol Biotechnol* 2019;**35**:26. https://doi.org/10.1007/s11274-019-2598-9
21. Gallagher RR, Patel JR, Interiano AL *et al.* Multilayered genetic safeguards limit growth of microorganisms to defined environments. *Nucleic Acids Res* 2015;**43**:1945–54. https://doi.org/10.1093/nar/gku1378
22. Chan CTY, Lee JW, Cameron DE *et al.* 'Deadman' and 'Passcode' microbial kill switches for bacterial containment. *Nat Chem Biol* 2016;**12**:82–6. https://doi.org/10.1038/nchembio.1979
23. Rottinghaus AG, Ferreiro A, Fishbein SRS *et al.* Genetically stable CRISPR-based kill switches for engineered microbes. *Nat Commun* 2022;**13**:672. https://doi.org/10.1038/s41467-022-28163-5
24. Steidler L, Neirynck S, Huyghebaert N *et al.* Biological containment of genetically modified *lactococcus lactis* for intestinal delivery of human interleukin 10. *Nat Biotechnol* 2003;**21**:785–9. https://doi.org/10.1038/nbt840
25. Asin-Garcia E, Batianis C, Li Y *et al.* Phosphite synthetic auxotrophy as an effective biocontainment strategy for the industrial chassis *Pseudomonas putida*. *Microb Cell Fact* 2022;**21**:156. https://doi.org/10.1186/s12934-022-01883-5
26. Chang T, Ding W, Yan S *et al.* A robust yeast biocontainment system with two-layered regulation switch dependent on unnatural amino acid. *Nat Commun* 2023;**14**:6487. https://doi.org/10.1038/s41467-023-42358-4
27. Hayashi N, Lai Y, Fuerte-Stone J *et al.* Cas9-assisted biological containment of a genetically engineered human commensal bacterium and genetic elements. *Nat Commun* 2024;**15**:2096. https://doi.org/10.1038/s41467-024-45893-w
28. Liu H, Zhang L, Wang W *et al.* An intelligent synthetic bacterium for chronological toxicant detection, biodegradation, and its subsequent suicide. *Adv Sci* 2023;**10**:2304318. https://doi.org/10.1002/advs.202304318
29. Arnolds KL, Dahlin LR, Ding L *et al.* Biotechnology for secure biocontainment designs in an emerging bioeconomy. *Curr Opin Biotechnol* 2021;**71**:25–31. https://doi.org/10.1016/j.copbio.2021.05.004
30. Piraner DI, Abedi MH, Moser BA *et al.* Tunable thermal bioswitches for *in vivo* control of microbial therapeutics. *Nat Chem Biol* 2017;**13**:75–80. https://doi.org/10.1038/nchembio.2233
31. Stirling F, Bitzan L, O'Keefe S *et al.* Rational design of evolutionarily stable microbial kill switches. *Mol Cell* 2017;**68**:686–697.e3. https://doi.org/10.1016/j.molcel.2017.10.033
32. Caliando BJ, Voigt CA. Targeted DNA degradation using a CRISPR device stably carried in the host genome. *Nat Commun* 2015;**6**:6989. https://doi.org/10.1038/ncomms7989
33. Ahrenholtz I, Lorenz MG, Wackernagel W. A conditional suicide system in *Escherichia coli* based on the intracellular degradation of DNA. *Appl Environ Microb* 1994;**60**:3746–51. https://doi.org/10.1128/aem.60.10.3746-3751.1994
34. Recorbet G, Robert C Fau - Givaudan A, Givaudan A Fau - Kudla B *et al.* Conditional suicide system of *Escherichia coli* released into soil that uses the *Bacillus subtilis sacB* gene. *Appl Environ Microb* 1993;**59**:1361–6. https://doi.org/10.1128/aem.59.5.1361-1366.1993
35. Babich H, Davis DL. Phenol: a review of environmental and health risks. *Regul Toxicol Pharm* 1981;**1**:90–109. https://doi.org/10.1016/0273-2300(81)90071-4
36. Wang Y, Meng F, Li H *et al.* Biodegradation of phenol by *isochrysis galbana* screened from eight species of marine microalgae: growth kinetic models, enzyme analysis and biodegradation pathway. *J Appl Phycol* 2019;**31**:445–55. https://doi.org/10.1007/s10811-018-1517-z
37. Duraisamy P, Sekar J, Arunkumar AD *et al.* Kinetics of phenol biodegradation by heavy metal tolerant rhizobacteria *glutamicibacter nicotianae* MSSRFPD35 from distillery effluent contaminated soils. *Front Microbiol* 2020;**11**:1573. https://doi.org/10.3389/fmicb.2020.01573
38. Roell GW, Carr RR, Campbell T *et al.* A concerted systems biology analysis of phenol metabolism in *Rhodococcus opacus* PD630. *Metab Eng* 2019;**55**:120–30. https://doi.org/10.1016/j.ymben.2019.06.013
39. Benkhennouche-Bouchene H, Mahy JG, Lambert SD *et al.* Statistical modeling and optimization of *Escherichia coli* growth parameters for the biological treatment of phenol. *Biocatal Agric Biotechnol* 2021;**34**:102016. https://doi.org/10.1016/j.bcab.2021.102016
40. Li CM, Wu HZ, Wang YX *et al.* Enhancement of phenol biodegradation: metabolic division of labor in co-culture of *Stenotrophomonas* sp. N5 and *advenella* sp. B9. *J Hazard Mater* 2020;**400**:123214. https://doi.org/10.1016/j.jhazmat.2020.123214
41. Vo PLH, Ronda C, Klompe SE *et al.* CRISPR RNA-guided integrases for high-efficiency, multiplexed bacterial genome engineering. *Nat Biotechnol* 2021;**39**:480–9. https://doi.org/10.1038/s41587-020-00745-y
42. Sung M, Yoo SM, Jun R *et al.* Optimization of phage λ promoter strength for synthetic small regulatory RNA-based metabolic engineering. *Biotechnol Bioproc E* 2016;**21**:483–90. https://doi.org/10.1007/s12257-016-0245-y
43. Elowitz MB, Leibler S. A synthetic oscillatory network of transcriptional regulators. *Nature* 2000;**403**:335–8. https://doi.org/10.1038/35002125
44. Prindle A, Samayoa P, Razinkov I *et al.* A sensing array of radically coupled genetic 'biopixels'. *Nature* 2012;**481**:39–44. https://doi.org/10.1038/nature10722
45. Marguet P, Tanouchi Y, Spitz E *et al.* Oscillations by minimal bacterial suicide circuits reveal hidden facets of host-circuit physiology. *PLoS One* 2010;**5**:e11909. https://doi.org/10.1371/journal.pone.0011909
46. Ren J, Nong NT, Lam Vo PN *et al.* Rational design of high-efficiency synthetic small regulatory RNAs and their application in robust genetic circuit performance through tight control of leaky gene expression. *ACS Synth Biol* 2024;**13**:3256–67. https://doi.org/10.1021/acssynbio.4c00323
47. Vo PNL, Lee H-M, Ren J *et al.* Optimized expression of hfq protein increases *Escherichia coli* growth. *J Biol Eng* 2021;**15**:7. https://doi.org/10.1186/s13036-021-00260-x
48. Peng F, Liu J, Ping J *et al.* An effective strategy for biodegradation of high concentration phenol in soil via biochar-immobilized *Rhodococcus pyridinivorans* B403. *Environ Sci Pollut Res* 2024;**31**:33752–62. https://doi.org/10.1007/s11356-024-33386-8
49. Gong T, Liu R, Zuo Z *et al.* Metabolic engineering of *Pseudomonas putida* KT2440 for complete mineralization of methyl parathion and γ-hexachlorocyclohexane. *ACS Synth Biol* 2016;**5**:434–42. https://doi.org/10.1021/acssynbio.6b00025
50. Liu Y, Zhang H, He X *et al.* Genetically engineered methanotroph as a platform for bioaugmentation of chemical pesticide contaminated soil. *ACS Synth Biol* 2021;**10**:487–94. https://doi.org/10.1021/acssynbio.0c00532
51. Pyong-Kyun S, Eun-Joo J. Effects of various parameters on biodegradation of degradable polymers in soil. *J Microbiol Biotechnol* 1999;**9**:784–8.
52. Lee J, Kim HS, Jo HY *et al.* Revisiting soil bacterial counting methods: optimal soil storage and pretreatment methods and comparison of culture-dependent and -independent methods.

PLoS One 2021;**16**:e0246142. https://doi.org/10.1371/journal.pone.0246142
53. Pepper I, Gerba CP, Gentry T *et al. Environmental Microbiology*, Vol. **3**. San Diego (CA): Academic Press, 2015. https://doi.org/10.1016/C2011-0-05029-9
54. Gillespie DT. Stochastic simulation of chemical kinetics. *Annu Rev Phys Chem* 2007;**58**:35–55. https://doi.org/10.1146/annurev.physchem.58.032806.104637
55. Maratea D, Young K, Young R. Deletion and fusion analysis of the phage φX174 lysis gene *E*. *Gene* 1985;**40**:39–46. https://doi.org/10.1016/0378-1119(85)90022-8
56. Bremer H, Yuan D. RNA chain growth-rate in *Escherichia coli*. *J Mol Biol* 1968;**38**:163–80. https://doi.org/10.1016/0022-2836(68)90404-X
57. Vogel U, Jensen KF. The RNA chain elongation rate in *Escherichia coli* depends on the growth rate. *J Bacteriol* 1994;**176**:2807–13. https://doi.org/10.1128/jb.176.10.2807-2813.1994
58. Bremer H, Dennis Patrick P. Modulation of chemical composition and other parameters of the cell at different exponential growth rates. *EcoSal Plus* 2008;**3**. https://doi.org/10.1128/ecosal.5.2.3
59. Jana NK, Roy S, Bhattacharyya B *et al.* Amino acid changes in the repressor of bacteriophage lambda due to temperature-sensitive mutations in its *cI* gene and the structure of a highly temperature-sensitive mutant repressor. *Protein Eng Des Sel* 1999;**12**:225–33. https://doi.org/10.1093/protein/12.3.225
60. Dirla S, Chien JYH, Schleif R. Constitutive mutations in the *Escherichia coli* AraC protein. *J Bacteriol* 2009;**191**:2668–74. https://doi.org/10.1128/jb.01529-08
61. Nistala GJ, Wu K, Rao CV *et al.* A modular positive feedback-based gene amplifier. *J Biol Eng* 2010;**4**:4. https://doi.org/10.1186/1754-1611-4-4
62. Ho JML, Miller CA, Parks SE *et al.* A suppressor tRNA-mediated feedforward loop eliminates leaky gene expression in bacteria. *Nucleic Acids Res* 2021;**49**:e25. https://doi.org/10.1093/nar/gkaa1179
63. Nielsen AAK, Segall-Shapiro TH, Voigt CA. Advances in genetic circuit design: novel biochemistries, deep part mining, and precision gene expression. *Curr Opin Chem Biol* 2013;**17**:878–92. https://doi.org/10.1016/j.cbpa.2013.10.003
64. Brophy JAN, Voigt CA. Principles of genetic circuit design. *Nat Methods* 2014;**11**:508–20. https://doi.org/10.1038/nmeth.2926
65. Baumann RJ, Bohme EH, Wiseman JS *et al.* Inhibition of *Escherichia coli* growth and diaminopimelic acid epimerase by 3-chlorodiaminopimelic acid. *Antimicrob Agents Chemother* 1988;**32**:1119–23. https://doi.org/10.1128/aac.32.8.1119
66. Xu J-Z, Ruan H-Z, Liu L-M *et al.* Overexpression of thermostable meso-diaminopimelate dehydrogenase to redirect diaminopimelate pathway for increasing L-lysine production in *Escherichia coli*. *Sci Rep* 2019;**9**:2423. https://doi.org/10.1038/s41598-018-37974-w
67. Chatterjee B, Mondal D, Bera S. Diaminopimelic acid and its analogues: synthesis and biological perspective. *Tetrahedron* 2021;**100**:132403. https://doi.org/10.1016/j.tet.2021.132403
68. Zheng L-Y, Liu N-H, Zhong S *et al.* Diaminopimelic acid metabolism by *Pseudomonadota* in the ocean. *Microbiol Spectr* 2022;**10**:e00691-22. https://doi.org/10.1128/spectrum.00691-22
69. Wilson DJ. NIH guidelines for research involving recombinant DNA molecules. *Account Res* 1993;**3**:177–85. https://doi.org/10.1080/08989629308573848
70. Zhao M, Yuan Z, Wu L *et al.* Precise prediction of promoter strength based on a *de novo* synthetic promoter library coupled with machine learning. *ACS Synth Biol* 2022;**11**:92–102. https://doi.org/10.1021/acssynbio.1c00117
71. Balzer S, Kucharova V, Megerle J *et al.* A comparative analysis of the properties of regulated promoter systems commonly used for recombinant gene expression in *Escherichia coli*. *Microb Cell Fact* 2013;**12**:26. https://doi.org/10.1186/1475-2859-12-26
72. Cebolla A, Vázquez ME, Palomares AJ. Expression vectors for the use of eukaryotic luciferases as bacterial markers with different colors of luminescence. *Appl Environ Microb* 1995;**61**:660–8. https://doi.org/10.1128/aem.61.2.660-668.1995
73. McClure WR. Rate-limiting steps in RNA chain initiation. *Proc Natl Acad Sci USA* 1980;**77**:5634–8. https://doi.org/10.1073/pnas.77.10.5634
74. Temme K, Hill R, Segall-Shapiro TH *et al.* Modular control of multiple pathways using engineered orthogonal T7 polymerases. *Nucleic Acids Res* 2012;**40**:8773–81. https://doi.org/10.1093/nar/gks597
75. Du F, Liu Y-Q, Xu Y-S *et al.* Regulating the T7 RNA polymerase expression in *E. coli* BL21 (DE3) to provide more host options for recombinant protein production. *Microb Cell Fact* 2021;**20**:189. https://doi.org/10.1186/s12934-021-01680-6
76. Tan S-I, Ng IS. New insight into plasmid-driven T7 RNA polymerase in *Escherichia coli* and use as a genetic amplifier for a biosensor. *ACS Synth Biol* 2020;**9**:613–22. https://doi.org/10.1021/acssynbio.9b00466
77. Kim B, Park H, Na D *et al.* Metabolic engineering of *Escherichia coli* for the production of phenol from glucose. *Biotechnol J* 2014;**9**:621–9. https://doi.org/10.1002/biot.201300263
78. Xu G, Wu A, Xiao L *et al.* Enhancing butanol tolerance of *Escherichia coli* reveals hydrophobic interaction of multi-tasking chaperone SecB. *Biotechnol Biofuels* 2019;**12**:164. https://doi.org/10.1186/s13068-019-1507-7
79. Zhang F, Qian X, Si H *et al.* Significantly improved solvent tolerance of *Escherichia coli* by global transcription machinery engineering. *Microb Cell Fact* 2015;**14**:175. https://doi.org/10.1186/s12934-015-0368-4
80. Ullers RS, Luirink J, Harms N *et al.* SecB is a bona fide generalized chaperone in *Escherichia coli*. *Proc Natl Acad Sci USA* 2004;**101**:7583–8. https://doi.org/10.1073/pnas.0402398101
81. Baars L, Ytterberg AJ, Drew D *et al.* Defining the role of the *Escherichia coli* chaperone SecB using comparative proteomics. *J Biol Chem* 2006;**281**:10024–34. https://doi.org/10.1074/jbc.M509929200
82. Sala A, Bordes P, Genevaux P. Multitasking SecB chaperones in bacteria. *Front Microbiol* 2014;**5**:666. https://doi.org/10.3389/fmicb.2014.00666
83. Randall LL, Hardy SJS. SecB, one small chaperone in the complex milieu of the cell. *Cell Mol Life Sci* 2002;**59**:1617–23. https://doi.org/10.1007/PL00012488
84. Kumar A, Grimes B, Fujita N *et al.* Role of the sigma70 subunit of *Escherichia coli* RNA polymerase in transcription activation. *J Mol Biol* 1994;**235**:405–13. https://doi.org/10.1006/jmbi.1994.1001
85. Gottesman S. Trouble is coming: signaling pathways that regulate general stress responses in bacteria. *J Biol Chem* 2019;**294,31**:11685–700. https://doi.org/10.1074/jbc.REV119.005593
86. Engl C, Jovanovic G, Brackston RD *et al.* The route to transcription initiation determines the mode of transcriptional bursting in *E. coli*. *Nat Commun* 2020;**11**:2422. https://doi.org/10.1038/s41467-020-16367-6
87. Wang B, Xu J, Gao J *et al.* Construction of an *Escherichia coli* strain to degrade phenol completely with two modified metabolic modules. *J Hazard Mater* 2019;**373**:29–38. https://doi.org/10.1016/j.jhazmat.2019.03.055
88. Van Schie PM, Young LY. Biodegradation of phenol: mechanisms and applications. *Biorem J* 2000;**4**:1–18. https://doi.org/10.1080/10588330008951128
89. Feist Cf Fau - Hegeman GD, Hegeman GD. Phenol and benzoate metabolism by *Pseudomonas putida*: regulation of tangential pathways. *J Bacteriol* 1969;**100**:869–77. https://doi.org/10.1128/jb.100.2.869-877.1969
90. Yan Q, Fong SS. Study of *in vitro* transcriptional binding effects and noise using constitutive promoters combined with UP

element sequences in *Escherichia coli*. *J Biol Eng* 2017;**11**:33. https://doi.org/10.1186/s13036-017-0075-2
91. Jia X, Zhang S, Li J *et al.* Engineered bacterial biofloc formation enhancing phenol removal and cell tolerance. *Appl Microbiol Biotechnol* 2020;**104**:1187–99. https://doi.org/10.1007/s00253-019-10289-0
92. Nandy S, Arora U, Tarar P *et al.* Monitoring the growth, survival and phenol utilization of the fluorescent-tagged *Pseudomonas oleovorans* immobilized and free cells. *Bioresour Technol* 2021;**338**:125568. https://doi.org/10.1016/j.biortech.2021.125568
93. Li Y, Li J, Wang C *et al.* Growth kinetics and phenol biodegradation of psychrotrophic *Pseudomonas putida* LY1. *Bioresour Technol* 2010;**101**:6740–4. https://doi.org/10.1016/j.biortech.2010.03.083
94. Mohammad SH, Bhukya B. Biotransformation of toxic lignin and aromatic compounds of lignocellulosic feedstock into eco-friendly biopolymers by *Pseudomonas putida* KT2440. *Bioresour Technol* 2022;**363**:128001. https://doi.org/10.1016/j.biortech.2022.128001
95. Zhang S, An Z, Su X *et al.* Phenol degradation at high salinity by a resuscitated strain *Pseudomonas* sp. SAS26: kinetics and pathway. *J Environ Chem Eng* 2023;**11**:110182. https://doi.org/10.1016/j.jece.2023.110182
96. Yoneda A, Henson WR, Goldner NK *et al.* Comparative transcriptomics elucidates adaptive phenol tolerance and utilization in lipid-accumulating *rhodococcus opacus* PD630. *Nucleic Acids Res* 2016;**44**:2240–54. https://doi.org/10.1093/nar/gkw055
97. Halvorsen TM, Ricci DP, Park DM *et al.* Comparison of kill switch toxins in plant-beneficial *Pseudomonas fluorescens* reveals drivers of lethality, stability, and escape. *ACS Synth. Biol.* 2022;**11**:3785–96. https://doi.org/10.1021/acssynbio.2c00386
98. Wright O, Delmans M, Stan G-B *et al.* GeneGuard: a modular plasmid system designed for biosafety. *ACS Synth. Biol.* 2015;**4**:307–16. https://doi.org/10.1021/sb500234s
99. You L, Cox RS, Weiss R *et al.* Programmed population control by cell–cell communication and regulated killing. *Nature* 2004;**428**:868–71. https://doi.org/10.1038/nature02491
100. Khraisheh M, Al-Ghouti MA, AlMomani F. *P. putida* as biosorbent for the remediation of cobalt and phenol from industrial waste wastewaters. *Environ Technol Innov* 2020;**20**:101148. https://doi.org/10.1016/j.eti.2020.101148
101. Henson WR, Hsu F-F, Dantas G *et al.* Lipid metabolism of phenol-tolerant *Rhodococcus opacus* strains for lignin bioconversion. *Biotechnol Biofuels* 2018;**11**:339. https://doi.org/10.1186/s13068-018-1337-z
102. Balseiro-Romero M, Monterroso C, Kidd PS *et al.* Modelling the *ex situ* bioremediation of diesel-contaminated soil in a slurry bioreactor using a hydrocarbon-degrading inoculant. *J Environ Manage* 2019;**246**:840–8. https://doi.org/10.1016/j.jenvman.2019.06.034
103. Meyer AJ, Segall-Shapiro TH, Glassey E *et al.* *Escherichia coli* "Marionette" strains with 12 highly optimized small-molecule sensors. *Nat Chem Biol* 2019;**15**:196–204. https://doi.org/10.1038/s41589-018-0168-3
104. Mairhofer J, Wittwer A, Cserjan-Puschmann M *et al.* Preventing T7 RNA polymerase read-through transcription—a synthetic termination signal capable of improving bioprocess stability. *ACS Synth. Biol.* 2015;**4**:265–73. https://doi.org/10.1021/sb5000115
105. Tickman BI, Burbano DA, Chavali VP *et al.* Multi-layer CRISPRa/i circuits for dynamic genetic programs in cell-free and bacterial systems. *Cell Syst* 2022;**13**:215–29. https://doi.org/10.1016/j.cels.2021.10.008
106. Li M, Gong L, Cheng F *et al.* Toxin-antitoxin RNA pairs safeguard CRISPR–Cas systems. *Science* 2021;**372**:eabe5601. https://doi.org/10.1126/science.abe5601
107. Choi Y-N, Kim D, Lee S *et al.* Quadruplet codon decoding-based versatile genetic biocontainment system. *Nucleic Acids Res* 2025;**53**:gkae1292. https://doi.org/10.1093/nar/gkae1292

Received: April 6, 2025. **Revised:** July 1, 2025. **Editorial Decision:** July 2, 2025. **Accepted:** July 8, 2025